A New Method to Reconstruct Quantitative Food Webs and Nutrient Flows from Isotope Tracer Addition Experiments

Andres Lopez-Sepulcre, Matthieu Bruneaux, Sarah M. Collins, Rana El-Sabaawi, Alexander S. Flecker, Steven A. Thomas

A new method to reconstruct quantitative food webs and nutrient flows from isotope tracer addition experiments

Andrés López-Sepulcre[1,2,3*], Matthieu Bruneaux[2], Sarah M. Collins[4], Rana El-Sabaawi[5], Alexander S. Flecker[6], and Steven A. Thomas[7]

[1]Department of Biology, Washington University in St. Louis, MO, USA

[2]Department of Biological and Environmental Sciences, University of Jyväskylä, Finland

[3]CNRS UMR 7618, Institute of Ecology and Environmental Sciences of Paris (iEES), Sorbonne Université, France

[4]Department of Zoology and Physiology, University of Wyoming, USA

[5]Department of Biology, University of Victoria, Canada

[6]Department of Ecology and Evolutionary Biology, Cornell University, USA

[7]School of Natural Resources, University of Nebraska-Lincoln, USA

[*]Corresponding author. E-mail: `alopezsepulcre@wustl.edu`

Abstract

Understanding how nutrients flow through food webs is central in ecosystem ecology. Tracer addition experiments are powerful tools to reconstruct nutrient flows by adding an isotopically enriched element into an ecosystem, and tracking its fate through time. Historically, the design and analysis of tracer studies have varied widely, ranging from descriptive studies to modeling approaches of varying complexity. Increasingly, isotope tracer data is being used to compare ecosystems and analyze experimental manipulations. Currently, a formal statistical framework for analyzing such experiments is lacking, making it impossible to calculate the estimation errors associated with the model fit, the interdependence of compartments, or the uncertainty in the diet of consumers. In this paper we develop a method based on Bayesian Hidden Markov Models, and apply it to the analysis of ^{15}N-NH_4^+ tracer additions in two Trinidadian streams in which light was experimentally manipulated. Through this case study, we illustrate how to estimate N fluxes between ecosystem compartments, turnover rates of N within those compartments, and the associated uncertainty. We also show how the method can be used to compare alternative models of food web structure, calculate the error arround derived parameters, and make statistical comparisons between sites or treatments.

Keywords: food webs, HMM, isotope tracer addition, model selection, nutrient uptake, state-space models

Une nouvelle méthode de reconstruction quantitative des réseaux trophiques et des flux de nutriments à partir d'expériences d'ajout de traceurs isotopiques

Abstract

Comprendre la manière dont les nutriments circulent au sein des réseaux trophiques est essentiel en écologie des écosystèmes. Les expériences d'ajout de traceur – consistant à ajouter un élément présentant un enrichissement isotopique dans un écosystème et à suivre son devenir au cours du temps – constituent un outil puissant pour reconstruire les flux de nutriments. Historiquement, ces données ont été analysées en recourant à méthodes diverses, allant d'études descriptives jusqu'à des modélisations plus ou moins complexes. Les données de traceurs isotopiques sont de plus en plus utilisées pour comparer des écosystèmes et analyser des manipulations expérimentales. Actuellement, il n'existe toujours pas de cadre statistique formel pour analyser ce type de données, ce qui rend impossible le calcul des erreurs d'estimation associées avec l'ajustement des modèles, de l'interdépendance des compartiments, ou encore de l'incertitude des régimes alimentaires des consommateurs. Dans cet article, nous présentons une méthode bayésienne basée sur des modèles de Markov cachés, et nous l'appliquons à l'analyse d'ajouts du traceur ^{15}N-NH_4^+ dans deux cours d'eau de l'île de la Trinité dans lesquels l'exposition lumineuse a été manipulée expérimentalement. Dans cette étude, nous montrons comment estimer les flux d'azote entre les compartiments de l'écosystème, les taux de renouvellement d'azote au sein de ces compartiments et les incertitudes associées. Nous montrons également que cette méthode peut être utilisée pour comparer des modèles de structures alternatives de réseaux trophiques, calculer l'erreur des paramètres dérivés, et réaliser des comparaisons statistiques entre des sites ou des traitements.

Introduction

Food webs are the cornerstone of community and ecosystem ecology because they describe the flow of matter and energy among organisms, thus defining important properties of an ecosystem such as stability and productivity (Paine, 1980; Rooney and McCann, 2012; Newbold et al., 1983; Carpenter et al., 2005). They provide the raw material for many ecological questions including the study of trophic cascades, nutrient cycling, and ecosystem productivity. Food web studies have been a major theme in ecological research for over a century, beginning with early work that identified trophic linkages (Elton, 1927). More recent studies have attempted to quantitatively track the movement of energy and materials through food web compartments, which remains particularly challenging because of complex methods for both data collection and analysis (Dodds et al., 2014).

While interaction strength has been defined in a variety of ways throughout the literature, ecosystem scientists are often interested in the biomass flux of a given nutrient between two species or compartments (Berlow et al., 2004). Researchers have used a variety of approaches to estimate trophic fluxes in the past, including gut-content analysis (Ledger et al., 2013), and analysis of egested material (such as faeces or pellets; Lima et al. 2002; Roslin and Majaneva 2016). These methods, however, are sensitive to sampling effects (Banašek-Richter et al., 2004), and only consider what is ingested, rarely accounting for what is assimilated into tissue, and therefore may not provide accurate estimates of how matter and energy flows through an ecosystem. Another approach is stable isotope analysis (SIA), which uses natural variation in the abundance of stable isotopes (most often ^{13}C, ^{15}N, or ^{2}H) across organisms to infer trophic relations (Peterson and Fry, 1987; Boecklen et al., 2011). While these natural abundance isotope webs offer a more integrative picture of diet, and directly target assimilated nutrients, they are often descriptive and unable to quantify fluxes. Moreover, results are sensitive to the assumptions of

diet mixing models (Post, 2002; Bond and Diamond, 2011), and often fail to differentiate carbon sources in freshwater ecosystems (Jardine et al., 2014). A powerful alternative is using whole-ecosystem isotope addition experiments to estimate fluxes across trophic compartments, and characterize nutrient cycles (Newbold et al., 1983; Kling, 1994; Carpenter et al., 2005).

Isotope tracer additions use small amounts of isotopically enriched nutrients to track the movement of nutrient tracers among different ecosystem compartments through time. Depending on the properties of the ecosystem, isotopes are added all at once (pulse design) or at a constant rate over a period of time (press design). The pulse design was used in early additions of radioisotopes to lakes (Hutchinson and Bowen, 1950; Rigler, 1956), streams (Ball and Hooper, 1963; Elwood and Nelson, 1972; Newbold et al., 1983), and meso- and micro-cosms (Whittaker, 1961; Patten and Witkamp, 1967). Whittaker (1961) pioneered the use of a linear donor-controlled compartment model to quantify transfers of the tracer through the food web, an approach also applied by Patten and Witkamp (1967) and Newbold et al. (1983). For their whole-stream addition of ^{32}P, Newbold et al. (1983) calculated transfer fluxes of the naturally occurring phosphorus from the steady-state solution of the compartment model. In press additions, the tracer accumulates in specific ecosystem compartments until an equilibrium state is achieved or the addition ends. Once the addition stops, the tracer begins to clear from basal compartments (e.g. algae), and progressively after, from higher trophic levels. This design has been used extensively in stream ecosystems to estimate nutrient uptake and turnover (Dodds et al., 2000; Mulholland et al., 2000).

Complemented with estimates of compartment sizes (biomasses), isotopic additions allow for the estimation of nutrient uptake and turnover rates for all ecosystem compartments, as well as quantification of the fluxes between them (Dodds et al., 2000; Mulholland

et al., 2000). This tracer addition approach has been used to characterize a variety of systems, including nitrogen (^{15}N) in streams (summarized by Dodds et al. 2014) and forests (Goodale et al., 2015), carbon (^{13}C) in marine and lake ecosystems (Middelburg et al., 2000; Cole et al., 2002; Pace et al., 2004), and deuterium-labeled water ($^{2}H_2O$) in terrestrial ecosystems (Kulmatiski et al., 2010).

Despite the increase in their use, there is no formal statistical framework to analyze whole-ecosystem data from tracer addition experiments. Instead, each trophic linkage is analyzed separately, solving for a mass balance between tracer uptake and turnover under the following assumptions: (1) the source pools from which a consumer obtains nutrients are known, (2) if there is more than one source, the proportional contribution of each source is known, (3) the added isotope is instantaneously and perfectly mixed within a compartment, and (4) consumers don't prey selectively within a source compartment i.e. the isotopic signature of the matter taken up reflects the signature of the source (Dodds et al., 2000; Mulholland et al., 2000). Some of these assumptions can be problematic. First, trophic links can be uncertain, and even when every consumer's source compartment is known, estimates of their proportional contribution tend to be crude approximations (Ainsworth et al., 2010). Second, consumers often differentially assimilate components of their diet, or selectively feed on specific portions of a sampled compartment. If not accounted for, this can cause seemingly paradoxical results, where consumers are more enriched with the tracer than the resource they feed on (Dodds et al., 2014). Regardless of their assumptions, neither of these approaches allows error in the inferences of parameters at lower trophic levels to propagate into flux estimates at higher trophic levels. Nor can they estimate and incorporate the error associated with uncertainty in trophic relationships or diet proportions. With the increase in the use of isotope tracer additions in comparative studies (Dodds et al., 2014; Norman et al., 2017; Tank et al., 2018) and ecosystem-scale

experiments (Collins et al., 2016; Whiles et al., 2013), it has become imperative to develop a statistical framework that allows rigorous comparisons among systems and treatments.

To meet this need, we developed a novel approach to the statistical analysis of isotope tracer data based on Bayesian Hidden Markov Models (Zucchini and MacDonald, 2009; King, 2014). Our approach allows for simultaneous modelling of nutrient transfers among all measured ecosystem compartments, providing estimations of parameter uncertainty that account for both observation and process error propagating across compartments. For omnivores, our method does not require *a priori* assumptions on the proportion of different prey constituting the diet, but rather estimates the proportion as a model parameter. It also allows the modeling of non-homogeneous compartments by estimating actively cycling vs. refractionary proportions, thus accounting for over-enriched signatures in consumers. Moreover, when there are doubts in the topology of the food web (e.g. whether a particular predator eats a specific prey or not), model comparison tools can be used to choose between the most parsimonious structure according to the data.

We first present the mathematical and statistical framework, framed as a Hidden Markov Model (HMM; Zucchini and MacDonald 2009), and then demonstrate its application with a case study on two Trinidadian montane streams differing in canopy cover (Collins et al., 2016). We illustrate how the approach can be used to (1) estimate model parameters, and their uncertainty, (2) calculate derived properties, such as nutrient fluxes and compartment residence times, and their uncertainty, (3) test alternative food web topologies, and (4) statistically compare experimental treatments.

Modeling tracer dynamics

Mathematical framework

The transfer of nutrients from one compartment to the other can be represented as a Markov Chain, a probabilistic model where the state of a given system (i.e. the distribution of nutrients across compartments) at time t depends only on its previous state at time $t-1$ (Iosifescu, 1980). In a HMM, dynamic data are modeled as a consequence of two stochastic processes: an unobserved biological process (here, nutrient fluxes), and an observation process that is conditional on the biological process (in our case, sampling and measurement of isotopic ratios). Table 1 shows a summary of the parameter notation followed and units of measurement used.

We conceptualize an ecosystem as a population of nutrient atoms flowing between compartments of an ecosystem. These compartments correspond, in HMM terminology, to the possible states a nutrient atom can be in. For a given ecosystem with a set of C compartments we can define the distribution of atoms among compartments at time t as a $C \times 1$ vector $\mathbf{x}^{(t)} = \{x_1^{(t)}, x_2^{(t)}, \ldots, x_N^{(t)}\}$, where $x_i^{(t)}$ indicates the number of nutrient atoms in compartment i at time t. We can then define a $C \times C$ transition matrix $\mathbf{\Psi}$ where each element $\psi_{i,j}$ defines the probability that an atom of nutrient in compartment j at time t finds itself in compartment i at time $t+1$. Some of the compartments, such the inorganic nutrient forms, may receive external inputs between t and $t+1$, which can be defined as non-zero elements in a $C \times 1$ vector of external inputs $\mathbf{y}^{(t)} = \{y_1^{(t)}, y_2^{(t)}, \ldots, y_N^{(t)}\}$ defined by input functions $f_i : t \rightarrow y_i^{(t)}$. Given this, we can project the distribution of nutrients from time t to $t+1$ using the equation:

$$\mathbf{x}^{(t+1)} = \mathbf{\Psi} \cdot \mathbf{x}^{(t)} + \mathbf{y}^{(t)} \tag{1}$$

This is a discretized form of the linear donor-controlled compartment model proposed by Mulholland and Keener (1974). The transition probabilities $\psi_{i,j}$ in $\mathbf{\Psi}$, are determined by two processes: nutrient uptake and nutrient loss. Uptake rates determine the probability that a nutrient atom moves from compartment j to i in one time step, and are defined as $\upsilon_{i,j} > 0$ for every pair of compartments where compartment i uses compartment j as a source of nutrient. Loss rates λ_j represent the probability that a nutrient atom leaves compartment j within one time step without being taken up by any other compartment, thus exiting the modeled ecosystem. The turnover rate k_j of a given compartment j (i.e. the proportion of nutrient exiting a given compartment per unit time) will be determined by the sum of the proportion consumed by other compartments, and the proportion lost λ_j:

$$k_j = \lambda_j + \sum_{i=1}^{C} \upsilon_{i,j} \tag{2}$$

In other words, Equation 1 is equivalent to stating that the nutrient dynamics of any given compartment j is described by the time-specific change in nutrient content Δx_j.

$$\Delta x_j^{(t)} = \sum_{1 \leq i \leq C, i \neq j} \upsilon_{j,i} x_j^{(t)} - k_j x_j^{(t)} + y_j^{(t)} \tag{3}$$

which can be simplified in the case where $y_j^{(t)} = 0$ (i.e. no external input for compartment j) to:

$$\Delta x_j^{(t)} = \sum_{1 \leq i \leq C, i \neq j} \upsilon_{j,i} x_j^{(t)} - k_j x_j^{(t)} \tag{4}$$

For example, let's consider a simple ecosystem with four compartments: an inorganic nutrient pool, a primary producer, a herbivore that consumes the primary producer, and an omnivore that feeds on both the primary consumer and the herbivore (Figure 1). Such

system would be defined by the following 4×4 transition matrix:

$$\mathbf{\Psi} = \begin{bmatrix} 1-k_1 & 0 & 0 & 0 \\ \upsilon_{2,1} & 1-k_2 & 0 & 0 \\ 0 & \upsilon_{3,2} & 1-k_3 & 0 \\ 0 & \upsilon_{4,2} & \upsilon_{4,3} & 1-k_4 \end{bmatrix} \tag{5}$$

and an exogenous input vector $\mathbf{y}^{(t)} = \{y_1^{(t)}, 0, 0, 0\}$. Note that if we assume the concentration of inorganic nutrient to be at a steady-state equilibrium ($x_1^{(t)} = x_1^{(t_0)}$ does not depend on time), it must fulfill that:

$$\forall t, \quad \frac{\Delta x_1^{(t)}}{\Delta t} = 0 \Longleftrightarrow y_1^{(t)} - k_1 x_1^{(t)} = 0 \tag{6}$$

$$\Longleftrightarrow y_1^{(t)} = (\upsilon_{2,1} + \lambda_1)\, x_1^{(t_0)} \tag{7}$$

thus y_1 does not depend on t. Note also that it is straightforward to modify these equations describing a discrete-time system to describe a continuous-time system. In this case, equation 1 becomes:

$$\frac{d\mathbf{x}^{(t)}}{dt} = \mathbf{\Psi} \cdot \mathbf{x}^{(t)} + \mathbf{y}^{(t)} \tag{8}$$

with $\mathbf{\Psi} \cdot \mathbf{x}^{(t)}$ and $\mathbf{y}^{(t)}$ describing instantaneous transition rates and input rates, respectively, instead of transition probabilities and input per time step. Equation 8 is basically a system of inhomogeneous linear differential equations (which simplifies into a homogeneous system if $\mathbf{y}^{(t)} = 0$). The transition matrix $\mathbf{\Psi}$ for a continuous-time model corresponding to the

ecosystem showed in Figure 1 becomes (compare with equation 5):

$$\mathbf{\Psi} = \begin{bmatrix} -k_1 & 0 & 0 & 0 \\ \upsilon_{2,1} & -k_2 & 0 & 0 \\ 0 & \upsilon_{3,2} & -k_3 & 0 \\ 0 & \upsilon_{4,2} & \upsilon_{4,3} & -k_4 \end{bmatrix} \tag{9}$$

The choice between a discrete and continuous model depends on the biology of the system under study. We use a continuous model in the case study of Trinidadian montane streams presented below.

In the case of tracer addition experiments, the aim is to increase the exogenous input of a tracer (or marked) nutrient population, and track the changes in the ratio between marked and unmarked nutrient (atomic ratio, in the case of isotope tracers). The addition of marked nutrient should cause a significant enrichment of the proportion of marked nutrient in water, yet a marginal increase in the total amount of nutrient in water. This can be achieved, for example, by using rare isotopic forms (e.g ^{15}N, ^{13}C, ^{18}O, or ^{2}H) that occur at extremely low proportion in nature. To model this, it is therefore necessary to follow two subpopulations of nutrient atoms: a tracer (or marked) population, usually the heavy isotopic form, and an unmarked population, defined by vectors $\mathbf{m}^{(t)} = \{m_1^{(t)}, \ldots, m_C^{(t)}\}$ and $\mathbf{n}^{(t)} = \{n_1^{(t)}, \ldots, n_C^{(t)}\}$ respectively, which add up to the total nutrient population $\mathbf{x}^{(t)} = \mathbf{n}^{(t)} + \mathbf{m}^{(t)}$. The proportion of tracer can then be defined as:

$$\mathbf{z}^{(t)} = \mathbf{m}^{(t)} \oslash \mathbf{x}^{(t)} \tag{10}$$

where $\oslash$ stands for the element-by-element division, also known as Hadamard division. Similarly, the exogenous input comprises marked $\mathbf{y_m}^{(t)}$ and unmarked $\mathbf{y_n}^{(t)}$ portions such

that $\mathbf{y^{(t)}} = \mathbf{y_n}^{(t)} + \mathbf{y_m}^{(t)}$. In a tracer addition experiment, the marked nutrient should be at much lower concentration than the unmarked nutrient such that $\mathbf{y_m}^{(t)} \ll \mathbf{y_n}^{(t)}$, and therefore $\mathbf{y}^{(t)} \approx \mathbf{y_n}^{(t)}$.

The schedule of tracer addition is reflected in the exogenous input vector of marked material $\mathbf{y_m}^{(t)}$, and usually consists of a period of increased input for one or two inorganic nutrient pools (e.g. NH_4^+ or NO_3^-) followed by a period of background input (although other experimental designs, such as repeated pulses, can be easily defined). The exogenous input for the unmarked population $\mathbf{y_n}^{(t)}$ is normally assumed constant.

Once we have an expected realization of the biological process model, the observation process can be modeled as sampling and measurement error around that expectation. The observed proportion of marked tracer in any given compartment i at time t can be modeled as a Gamma distribution, which fulfills the multiplicative properties of proportions and allows for the skewed distribution typical of low-concentration data. We parameterized the Gamma distributiom with the projected mean $z_i^{(t)}$ and a coefficient of variation η shared across compartments, such that the observed proportion $z_{\text{obs},i}^{(t)}$ follows (using Gamma* to denote the non-standard Gamma parameterization):

$$z_{\text{obs},i}^{(t)} \sim \text{Gamma}^* \left(z_i^{(t)}, \eta \right) \tag{11}$$

This is equivalent to modeling Gamma distributions with shape parameter $\alpha_i = \eta^{-2}$, and rate parameter $\beta_i = \left(z_i^{(t)} \cdot \eta^2 \right)^{-1}$. Although the Gamma distribution can hypothetically reach values larger than 1, the expected isotopic proportions are extremely low, and therefore the probability density for values higher than one is negligible.

We will assume the total biomass of nitrogen x_i in compartment i to be approximately constant throughout the experiment, following a truncated normal distribution. This assumes additive properties and allows for zero values of biomass, which can occur for a

given compartment in some sampling points. We note the truncated normal distribution with a mean $x_i^{(t0)}$ (the initial biomass of compartment i) and a compartment-specific standard deviation SD_i:

$$x_i^{(t)} \sim \mathrm{TNorm}_{\mathrm{lower}=0}\left(x_i^{(t0)}, \mathrm{SD}_i\right) \tag{12}$$

Over-enriched compartments

The model as formulated above assumes that the tracer is well mixed, and consumers do not selectively feed on differently labeled subcomponents of the source compartment. If this is true, the tracer signature of a consumer cannot exceed the signature of the source compartment. In practice, however, it is not uncommon for a consumer's isotopic label to be higher than its resource (Newbold et al., 1983; Dodds et al., 2014). This is because some compartments, particularly detrital ones, consist of material in which only a proportion is biologically active and assimilating tracer during the experiment. If consumers selectively feed on active constituents and/or preferentially assimilate active fractions their signature can become higher than the average of the resource compartment. For example, coarse benthic organic matter (CBOM) is largely biologically inactive, and nutrient uptake into leaf packs is associated with the biofilm surrounding it. While the average tracer signal measured on the whole compartment might be low, the biofilm can have a high tracer signature, and organisms selectively feeding on (or assimilating) that biofilm will become highly labeled.

In order to allow for this in the model, one can assume that the biomass of any given compartment i is split into two portions: an active and a refractory one. The active portion takes up nutrients throughout the experiment and contributes to changes in $x_i^{(t)}$ (both $m_i^{(t)}$ and $n_i^{(t)}$). The refractory portion has negligible nutrient uptake and turnover

within the timespan of the experiment, and thus does not contribute to changes in $x_i^{(t)}$. If we define a vector of active proportions for the C compartments $\pi = \{\pi_1, \ldots, \pi_C\}$ where $0 < \pi_i < 1$ whenever compartment i is assumed to be non-homogeneous, the apparent uptake rates $\upsilon'_{i,\cdot}$ and apparent turnover rate k'_i of the whole compartment will be:

$$\upsilon'_{i,\cdot} = \upsilon_{i,\cdot} \cdot \pi_i \tag{13}$$

$$k'_i = k_i \cdot \pi_i \tag{14}$$

In practice, this means that, while the biological model (Equation 5) runs only on the active portion of biomass, the observation model accounts for the total biomass. Newbold et al. (1983) preceded the present manuscript in recognizing that the standing stocks of the actively cycling components (as well as transfer fluxes) can be estimated from the model's steady-state solution. Note that π bears a similar meaning to the estimates of exchangeable P in Newbold et al. (1983) and the inverse of multiplier M in Dodds et al. (2014).

Model fitting

Fitting the above Hidden Markov Model requires time series of the observed tracer proportions $z_{\text{obs},i}^{(t)}$, in each compartment and data on compartment biomasses $x_{\text{obs},i}^{(t)}$. In isotope tracer studies, where there is a heavy isotope (the marked tracer) and a light (unmarked) isotope, the amount of marked tracer will often be expressed as δ-value. For example in studies of nitrogen dynamics, the tracer is ^{15}N (heavier than the naturally common ^{14}N), and data is obtained as δ^{15}N which, for any given compartment i at time t is:

$$\delta^{15}N_i^{(t)} = \left(\frac{R_i^{(t)}}{R_0} - 1 \right) \cdot 1000 \tag{15}$$

where $R_i^{(t)} = ({}^{15}N/{}^{14}N)_i^{(t)}$ is the isotopic ratio in compartment i at time t and R_0 is the isotopic ratio in a standard air sample (e.g. for ^{15}N this is taken to be 0.003663). In order to fit the above model to this data, it is necessary to convert the δ-values to observed proportions. This can be done by expressing $z_{\text{obs},i}^{(t)}$ as a function of $R_i^{(t)}$:

$$z_{\text{obs},i}^{(t)} = \frac{m_i^{(t)}}{n_i^{(t)} + m_i^{(t)}} = \frac{{}^{15}N_i^{(t)}}{{}^{14}N_i^{(t)} + {}^{15}N_i^{(t)}} = \frac{R_i^{(t)}}{R_i^{(t)} + 1}$$

and then using a rearrangement of Equation 15 to replace $R_i^{(t)}$ in the equation for $z_{\text{obs},i}^{(t)}$:

$$z_{\text{obs},i}^{(t)} = R_0 \left(\frac{\delta^{15}N_i^{(t)}}{1000} + 1 \right) \left[R_0 \left(\frac{\delta^{15}N_i^{(t)}}{1000} + 1 \right) + 1 \right]^{-1} \tag{16}$$

Given this data, and an assumed system topology denoting which compartment pairs are assumed to be linked as consumer and resource (i.e. which off-diagonal elements $\psi_{i,j} > 0$), we can fit the model to the data using a Bayesian framework. To do so, we need to define priors for all $\upsilon_{i,j} \geq 0$, $0 \leq \pi_i \leq 1$, λ_i, and η. These can be uninformative (i.e. flat) distributions within the parameter bounds, or informative priors if there is prior knowledge on these quantities. For parameters which are positive but for which no upper bound is known precisely a priori, a half-Cauchy distribution defined by its scale parameter (i.e. its median) is a reasonable choice. We used half-Cauchy priors for the uptake rates from the inorganic input compartments since those compartments are constantly being renewed with the stream flow. For uptake rates and loss rates from biotic compartments, we used (scaled) beta priors to impose a maximum rate while allowing to put more prior belief in small rate values: for example, it is unreasonable to allow uptake or loss rates greater than one with our data, since this would indicate a replacement of the whole nitrogen content of a biotic compartment within one day. Hence, we started our modelling approach with

the following weakly informative priors:

$$
\begin{aligned}
\upsilon_{i,j} &\sim \mathit{Half\text{-}Cauchy}(\mathit{scale} = 250) \text{ for input compartments } j \in \mathcal{I} \\
\upsilon_{i,j} &\sim \mathit{Beta}(\alpha = 1, \beta = 3, \mathit{scale} = 1) \text{ for all other uptake rates } \upsilon_{i,j} > 0 \\
\lambda_i &\sim \mathit{Beta}(\alpha = 1, \beta = 3, \mathit{scale} = 1) \\
\pi_i &\sim \mathit{Uniform}(0, 1) \text{ for all basal compartments } \pi_i < 1 \\
\eta &\sim \mathit{Half\text{-}Cauchy}(\mathit{scale} = 1)
\end{aligned}
$$

where $\mathcal{I}$ defines the set of inorganic nutrient compartments. We adjusted them for some parameters after realising from initial runs that they could be either too restrictive or too permissive, depending on the compartments:

$$
\begin{aligned}
\upsilon_{eudan,CBOM} &\sim \mathit{Beta}(\alpha = 1, \beta = 3, \mathit{scale} = 0.5) \\
\upsilon_{lepto,seston} &\sim \mathit{Beta}(\alpha = 1, \beta = 3, \mathit{scale} = 0.5)
\end{aligned}
$$

In the formulation above, we defines X as following a scaled beta distribution $\mathit{Beta}(\alpha, \beta, \mathit{scale})$ if X/scale follows a beta distribution $\mathit{Beta}(\alpha, \beta)$.

The likelihood $\mathcal{L}$ of each observation $z^{(t)}_{\text{obs},i}$ is given by Equation 11, and the joint log-likelihood of all observations, as the sum of logarithms of all individual likelihoods. To help identifiability, the model can be constrained so that the total nutrient biomass of each compartment x_i is randomly distributed with known constant mean and coefficient of variation cv_i as described in Equation 12. These values can be obtained from independent estimations of compartment-specific biomasses $x_{\text{obs},i}$. The likelihood of each biomass $x^{(t)}_i$ projected by the model is evaluated against this distribution at each time-point where there is any observation $z^{(t)}_{\text{obs},i}$, in order to constrain the biomass change of the system com-

partments in the model. The posterior distribution of the parameters can be obtained by sampling the product of prior and likelihood using Markov Chain Monte Carlo techniques (Geman and Geman, 1984).

Model selection, derived properties, and statistical comparisons

If there is uncertainty over the presence or absence of any given trophic link, it is possible to define and to fit alternative models representing different hypothesized food-web topologies $\mathbf{\Psi}_h$ differing in whether particular uptake rates $\upsilon_{i,j}$ are equal to 0 or not. The model fits can then be compared using the Deviance Information Criterion (DIC; Spiegelhalter et al. 2002), defined as:

$$\mathrm{DIC} = \bar{D} + p_D \tag{17}$$

where D is the set of deviance values calculated from the log-likelihood value at each MCMC iteration as $-2\times\log\mathcal{L}$, $\bar{D}$ is the mean deviance value and p_D is the effective number of parameters in the model and can be calculated as $var(D)/2$(Gelman et al., 2003). The most parsimonious model will be the one with the lowest DIC. A DIC difference ΔDIC greater than 2 indicates some evidence for the model with a lower DIC, while substantial evidence would be indicated by $\Delta\mathrm{DIC} > 5$. It is also possible to compare the proportional support for any given model $\mathbf{\Psi}_h$ as a DIC weight (Link and Barker, 2010):

$$w_h = \frac{e^{\Delta\mathrm{DIC}_h/2}}{\sum_{g=1}^{M} e^{\Delta\mathrm{DIC}_g/2}} \tag{18}$$

where h represents the model hypothesis in question, and M the total number of models tested.

Any derived metric of the system, such as total uptake and residence times of different compartments, or proportion of a given prey in a consumer's diet, can be calculated

using the MCMC chains of the parameter estimates involved in the calculations. This will produce an equally sized MCMC chain from which to create the distribution of the metric and its uncertainty (e.g. 95% credible intervals). Similarly, one can compare estimates of parameters or derived metrics between streams by subtracting (or dividing) the MCMC chains of the two estimates and producing a distribution and credible intervals of the difference in the estimates. The 95% credible intervals of statistically significant differences should not overlap 0 (or 1 for ratios).

Case study: nitrogen fluxes in Trinidadian montane streams

Study system and experimental methods

As an empirical illustration of our statistical modeling framework, we showcase its use in a case study conducted in Trinidadian streams, using simultaneous ^{15}N tracer isotope additions to evaluate the effects of an experimental manipulation of light availability on major food web fluxes. These experiments were carried out in streams of the Northern Range of Trinidad: Upper La Laja (UL) and Lower La Laja (LL). The study reaches are 100 and 156 meters long, respectively, and form part of a long-term experiment to study interactions betwen ecological and evolutionary processes (Travis et al., 2014). These data have been previously analyzed using current methodology in Collins et al. (2016), providing a good point of comparison between the current method and our proposed modelling.

Details of the experiment and sampling can be found in Collins et al. (2016). In summary, we established a continuous drip of a solution of ^{15}N labeled ammonium (as dissolved $^{15}NH_4Cl$) on the upstream end of each stream with a rate of 10 mL min^{-1} over a 10-day period from March 7-16, 2010. The N injections increased the $\delta^{15}N$ of dissolved

ammonium to approximately 20,000‰, yet the concentration of ammonium added was below 5% of ambient NH_4 and thus did not enrich the stream. We sampled biomass of food web compartments and water chemistry at approximately 15, 30 and 60m downstream, both in pool and riffle habitat, on days 3, 7 and 10 of the injection, and on days 13, 17, 20, 30 and 40 (post-injection). The sampled food web compartments include water chemistry (NH_4^+, and NO_3^-), basal resources (epilithon, seston, FBOM, and CBOM), eight common invertebrate taxa representing all major functional feeding groups including grazers (*Petrophila*, and *Psephenus*), filterers (*Leptonema*), collectors (*Tricorythodes*, *Phylloicus*, and *Eudaniela*), and predators *Argia*, and *Euthyplocia*). For simplicity, fish were not included in this illustrative analysis. For each of the 14 compartments we analyzed the isotopic ratio (δ^{15}N) of the samples obtained through time, and estimated the standing biomass of each compartment in mass of nitrogen per m^2 at two points in time. We also collected background samples from each compartment, either before the experiment or upstream from the injection, to estimate background isotopic values. We detail the analytical methods in the Appendix.

Model specification and selection

The Trinidadian stream web modelled is composed of the 14 compartments described above. Therefore, the distribution of nitrogen biomasses at any given time t is described by the vector

$$\mathbf{x}^{(t)} = \{x_{NH4}^{(t)}, x_{NO3}^{(t)}, x_{epi}^{(t)}, x_{ses}^{(t)}, x_{FBOM}^{(t)}, x_{CBOM}^{(t)}, x_{pet}^{(t)}, x_{pse}^{(t)}, x_{lep}^{(t)}, x_{tri}^{(t)}, x_{eud}^{(t)}, x_{phy}^{(t)}, x_{arg}^{(t)}, x_{eut}^{(t)}\}$$

which can be projected following the system of differential equations showed in Equation 8, given a transition matrix Ψ of trophic relationships. Given the uncertainty of some

trophic links, we test eight variations of the food web structure assumed by Collins et al. (2016), which corresponds to the matrix shown in Box 1.

Because the dynamics of the two inorganic element compartments, NH_4^+ and NO_3^- , occur at much faster rates than the rest, the system can be numerically approximated by assuming that they are completely regenerated at each infinitesimal time step and driven by external inputs or, in other words, that they are completely replaced by the flux from upstream. Note that this assumption does not imply that the system modelled is completely open, but is merely a mathematical simplification that treats water nutrient as a given in order to simplify the estimation. This can be mathematically expressed by setting $\psi_{1,1} = \psi_{2,2} = 0$ and by replacing after each step of the numerical integration of the system of differential equations the elements x_1 and x_2 of $\mathbf{x}$ by values that reflect the measured profiles for NH_4^+ and NO_3^- at sampling point s. In our example, we have three sampling points (transects) per stream.

Given this, we can model the two parallel subsystems comprising $\mathbf{x}$: unmarked nutrient $\mathbf{n}$ and marked nutrient $\mathbf{m}$, representing the dynamics of each isotope. While both systems will be governed by the same transition matrix $\mathbf{\Psi}$, they have different initial values $\mathbf{n}^{(0)}$ and $\mathbf{m}^{(0)}$ corresponding to the background isotopic ratios before the drip experiment has started. The inorganic nutrient compartments also have different forced input profiles between unmarked and marked nutrient pools. The forced quantity of unmarked tracer in the inorganic compartments is constant through time, such that:

$$n_i^{(s,t)} = {}^{14}N_{i,\text{bkg}}^{(s)} \quad \text{for } i \in \mathcal{I} \text{ and all } t \text{ values} \tag{19}$$

where $\mathcal{I}$ defines the set of inorganic nutrient compartments (NH_4^+ and NO_3^-) and ${}^{14}N_{i,\text{bkg}}^{(s)}$ is the natural (background) abundance of ${}^{14}N$ (in mgN/m^2) in the inorganic nutrient compartment i measured at sampling transect s.

On the contrary, the forced quantity of marked nutrient in the inorganic compartments changes with the experimental enrichment profile. This means that, if we define t_{off} as the time the drip is turned off, then the following step function drives $m_i^{(s,t)}$:

$$m_i^{(s,t)} = \begin{cases} {}^{15}N_{i,\text{bkg}}^{(s)} + {}^{15}N_{i,\text{add}}^{(s)} & \text{for } i \in \mathcal{I} \text{ and } t < t_{\text{off}} \\ {}^{15}N_{i,\text{bkg}}^{(s)} & \text{for } i \in \mathcal{I} \text{ and } t \geq t_{\text{off}} \end{cases} \tag{20}$$

Here, ${}^{15}N_{i,\text{bkg}}^{(s)}$ represents the natural (background) abundance of the heavy isotope (^{15}N) form of the inorganic nutrient compartment measured at sampling transect s before nutrient addition, and ${}^{15}N_{i,\text{add}}^{(s)}$ is the additional ^{15}N measured during the experimental addition at sampling transect s.

We tested eight topological model structures of the network $\mathbf{\Psi_h}$ representing the variations of $\mathbf{\Psi_{111}}$ where one or more of three uncertain links were eliminated. The uncertain links corresponded to the uptake of FBOM by the *Eudaniela* crabs, and predation of *Psephenus* waterpennies and *Petrophila* caterpillars by *Argia* damselflies (Table 2).

We fit the models to the data of Lower and Upper La Laja using transect and compartment specific time series of isotopic proportions $z_{\text{obs},i}^{(s,t)}$, as well as compartment-specific biomass data $x_{\text{obs},i}^{(s,t)}$ at three points in time t, and three points in space s. Latent biomasses x_i were assumed to be constant (i.e. at steady state), therefore considering sample differences as random observed variation cv_i. In practice, this allows for deviations of the steady state assumption that are within the range of the compartment's natural variation.

We fit the model in R version 3.6 (R Core Team, 2019) by implementing it in Stan (Carpenter et al., 2017) and running it with the RStan package (Stan Development Team, 2019). Details of the model implementation and of the priors used are described in the Supplementary Material S1. The data and the source code used in our study can be found as an R package at https://doi.org/10.5061/dryad.8sf7m0chx (Lopez-Sepulcre et al., 2020).

We assumed that both streams have the same network topology of trophic links, albeit with different parameter values. We therefore calculated the joint DIC for both streams by adding the DICs of the same model fit to the two streams. We chose the best model as the one with the lowest joint DIC.

Calculation of derived parameters

After selecting the best model, we illustrate the calculation of some important derived metrics, their uncertainty, and their comparison between the natural (LL) and open canopy (UL) streams. To do so, one only has to apply the required calculation with all 1000 sampled values of the MCMC chain rather than with the estimates of the parameters. This produces a probability distribution for the derived parameter, which can be used to calculate measures of dispersion such as standard errors or 95% quantiles (i.e. credible intervals).

A common quantity of interest is the expected residence or turnover time T_j of nutrient N in each compartment j, which can be calculated as the inverse of the turnover rate:

$$T_j = \frac{1}{k_j} = \frac{1}{\lambda_j + \sum_{i=1}^{C} \upsilon_{i,j}} \tag{21}$$

In the case of compartments divided into active and refractory subcompartments, the apparent residence time T'_j will be larger:

$$T'_j = \frac{1}{\pi_j k_j} = \frac{1}{\pi_j \left(\lambda_j + \sum_{i=1}^{C} \upsilon_{i,j}\right)} = \frac{T_j}{\pi_j} \tag{22}$$

The flux rates between compartments can be calculated as:

$$F_{i,j} = \upsilon_{i,j} \hat{X}_i \tag{23}$$

where $F_{i,j}$ represents the flux from compartment j to compartment i, and $\hat{X}_i$ is the expected biomass. Because we assume the system to be at steady state, expected biomasses can be calculated using eigen-analysis of the system as follows. Under steady state, the two nutrient forms NH_4^+ and NO_3^- ought to remain constant, which we can achieve by defining a transfer matrix $\mathbf{\Psi'}$ that equals $\mathbf{\Psi}$ but with $\psi'_{1,1} = \psi'_{2,2} = 1$. This matrix will have at least 2 right eigenvectors $\mathbf{v^{(NH4)}}$ and $\mathbf{v^{(NO3)}}$ corresponding to an eigenvalue of 1, and which are scaled to a norm of 1. The elements i of each of these 14×1 vectors represent the relative equilibrium biomass of compartment i that originates from each of the two inorganic nutrients, NH_4^+ and NO_3^-, respectively. Because the eigenvectors $\mathbf{v^{(NH4)}}$ and $\mathbf{v^{(NO3)}}$ are scaled to a norm of 1, they need to be rescaled based on the mass of NH_4^+ and NO_3^- in the water, respectively. The total equilibrium biomass $\hat{X}_i$ of compartment i at steady state can thus be calculated as the sum elements i of the two rescaled vectors as follows:

$$\hat{X}_i = x_1 \frac{\mathrm{v}_i^{(NH4)}}{\mathrm{v}_1^{(NH4)}} + x_2 \frac{\mathrm{v}_i^{(NO3)}}{\mathrm{v}_2^{(NO3)}} \tag{24}$$

where x_1 and x_2 are the background masses (in $\mathrm{mgN/m^2}$) of NH_4^+ and NO_3^- in the stream. It is worth noting that at steady state, it should be true that inputs should equal outputs, and therefore:

$$F_{i,\cdot} = k_i \cdot \hat{X}_i \iff \hat{X}_i = F_{i,\cdot} \cdot T_i \tag{25}$$

where $F_{i,\cdot}$ is the total flux through compartment i:

$$F_{i,\cdot} = \sum_{j=1}^{C} F_{i,j} \hat{X}_j \tag{26}$$

The total flux of N through the system can then be calculated as the sum of fluxes from the set of nutrient input compartments $\mathcal{I}$ (in our case, NH_4^+ and NO_3^-) and the set of basal

compartments $\mathcal{B}$ (in our case, epilithon, seston, FBOM and CBOM).

$$F_T = \sum_{i \in \mathcal{I}} \sum_{j \in \mathcal{B}} F_{i,j} \tag{27}$$

Total flux is of interest as an indicator of whole-ecosystem productivity, and we expect it to be higher under higher light conditions (i.e. in UL). A second metric of interest is the relative use of NO_3^- to NH_4^+ by primary producers. Primary producers favour NH_4^+ over NO_3^-, due to lower assimilation cost (Morris, 1974). Because more productive streams have higher demand of N and greater energy supply, we expect primary producers in the high light stream to supplement their N need by assimilating nitrate and therefore have a higher ratio of NO_3^- flux to NH_4^+ (Morris, 1974). The proportion of N uptake flux from two different sources can be calculated as:

$$P_{i,j}^U = \frac{\upsilon_{i,j} x_j}{\sum_{r=1}^{C} \upsilon_{i,r} x_r} \tag{28}$$

where i stands for the consumer and j for the source of which we want to calculate the proportion of each form taken up. We will calculate the proportional use of NO_3^- by epilithon $P_{\text{epi,NO3}}^U$ to test the above hypothesis of preferential NH_4^+ use under light limitation. Note that this can also be expressed as a ratio of NO_3^- to NH_4^+ use:

$$R_{\text{epi,NO3}} = \frac{P_{\text{epi,NO3}}^U}{1 - P_{\text{epi,NO3}}^U} \tag{29}$$

Similarly, one can use $P_{i,j}^U$ to evaluate the importance of a particular compartment in the diet of a consumer. We illustrate this by calculating the importance of *Petrophila* water moths in the diet of *Argia* damselflies $P_{\text{arg,pet}}^U$.

Conversely, we can calculate the contribution of a particular consumer i to the turnover

of a given resource compartment j as:

$$P_{i,j}^{K} = \frac{\upsilon_{i,j}}{k_j} = \frac{\upsilon_{i,j}}{\lambda_j + \sum_{r=1}^{C} \upsilon r, j} \tag{30}$$

As an example, we calculate the contribution of *Eudaniela* crabs to the turnover of CBOM, $P_{\text{eud,CBOM}}^{K}$.

Derived parameter uncertainty and statistical comparisons

One of the main advantages of Bayesian inference though MCMC is that it is straightforward to carry out the estimation error on the primary parameters onto the derived parameters. This is done by simply applying the relevant calculation elementwise on the MCMC chains of the estimated parameters. This results in a posterior distribution of the derived parameter that naturally accounts for the error in all its component parameters. One can then calculate from the posterior distribution any relevant measure of uncertainty (e.g. standard error or credible intervals).

In the same manner, one can compare the parameter estimates between two streams by simply calculating the elementwise difference (or ratio, or any other measure of effect size) in the MCMC chains. A Bayesian posterior predictive p-value for the difference can then be extracted by calculating the proportion of the posterior distribution that falls below 0 (or 1, in the case of a ratio).

Results

The most parsimonious network topology corresponded to model $\mathbf{\Psi}_{100}$, which includes the consumption of *Petrophila* by *Argia*, but not consumption of *Psephenus* by *Argia*, nor FBOM by *Eudaniela* crabs (Table 2). The second best model was 3.3 DIC units

away, indicating moderate support for the best model. However, the overall support for a *Petrophila* → *Argia* link is higher if we consider all tested models. The sum of the DIC weights of all the models including that link is 0.90 (out of 1), compared to only 0.19 for a *Psephenus* → *Argia* link, and <0.01 for an FBOM → *Eudaniela* link. We therefore present the results for model $\mathbf{\Psi}_{100}$. Figure 2 shows the fit for isotope ratios for this model in both streams for the first transects (see Figure S1 for all transects, and Figure S2 for biomass fit), while the parameter estimates, credible intervals, MCMC chains, and posterior distributions, can be found in the Table S1 and Figure S3).

In order to compare our proposed approach to current standard methodology, in Figure 3 we compare our estimates of Lower La Laja compartment fluxes and turnover times, with estimates obtained in a previous analysis of the same data (Collins et al., 2016), using current methodology (Dodds et al., 2000). For basal compartments that are split into an active portion π_i and a refractory portion $1 - \pi_i$, apparent turnover times T_i' in our analyses (Equation 22) are equivalent to the turnover times estimated in Collins et al. (2016). 14 of the 24 compartment uptake rates estimated by Collins et al. lie within the 95% credible intervals of our estimates, as 14 out of the 24 turnover time estimates do. Relative to the estimates derived by our model, the estimates of Collins et al. tend to overestimate uptake in the basal compartments and underestimate it for some consumers, while the converse is true for turnover time. Differences between methods in estimates were often not trivial, and in some cases varied by an order of magnitude (e.g. CBOM uptake or *Eudaniela* turnover). The negative relationship between the bias of uptake and turnover time is expected, given that an overestimate of uptake must be balanced by decreased turnover time in order to explain the same concentration of tracer in a given compartment.

The estimates and 95% credible intervals of all fluxes among compartments, turnover

times, and expected steady-state biomasses are found in the supplementary material (Tables S2 and S3) and represented in Figure 4. This figure summarizes the three main aspects of nitrogen dynamics across compartments: fluxes between compartments, turnover (or residence) times, and compartment biomasses. Basal compartments are divided into their active (solid white) and refractory (hatched) portions as estimated by π_i, with T_i and T_i' represented by the width of the white solid portion of the box, and the total width of the box, respectively. As expected, active portions of basal compartments tend to be larger in the open canopy stream than the closed canopy stream, particularly for epilithon ($(\pi_{\text{epi}})^{LL} = 0.13 \pm 0.07$; $(\pi_{\text{epi}})^{UL} = 0.44 \pm 0.12$) and CBOM ($(\pi_{\text{CBOM}})^{LL} = 0.30 \pm 0.14$; $(\pi_{\text{CBOM}})^{UL} = 0.50 \pm 0.13$; Table S1). Another clear and expected pattern that emerges from Figure 4 is the overall higher fluxes into the basal compartments in the open canopy stream. This is illustrated in Figure 5 and is in good part due to an increased NO_3^- uptake by epilithon and CBOM. In contrast, the increase in N uptake by FBOM, is mostly due to increased NH_4^+ uptake.

A consistent pattern across our analyses was the high uncertainty associated with estimates of fluxes, turnover, and other derived parameters. Despite this quantitative uncertainty, it is possible to make important statistical inferences regarding differences among compartments and between streams. Total flux is higher in the open canopy than the closed canopy stream, ($(F_T)^{UL} - (F_T)^{LL} = 63.7 \pm 35.9$, one-sided Bayesian p-value = 0.036, Figure 6A) and epilithon's uptake shows a higher ratio of NO_3^- to NH_4^+ uptake ($\log[(R_{\text{epi,NO3}})^{UL}] - \log[(R_{\text{epi,NO3}})^{LL}] = 3.54 \pm 1.51$, p = 0.008, Figure 6B), as expected. Although there seems to be a higher contribution of *Eudaniela* crabs to CBOM turnover in the closed canopy stream, the parameters around *Eudaniela* are highly uncertain due to irregular sampling (crabs captures are patchy), and this difference is not significant ($\text{logit}[(P^K_{\text{eud,CBOM}})^{UL}] - \text{logit}[(P^K_{\text{eud,CBOM}})^{LL}] = -1.02 \pm 1.74$, p = 0.28, Figure

6C). A clearer but still non significant result is that *Petrophila* moths seem to represent a higher proportion of the diet of *Argia* damselfiles in in our high light stream (UL > LL, $(\text{logit}[(P^{U}_{\text{arg,pet}})^{UL}] - \text{logit}[(P^{U}_{\text{arg,pet}})^{LL}]) = 1.48 \pm 1.43$, p = 0.13, Figure 6D).

Discussion

We have presented a statistical formalization of a tracer addition to track nutrient movement through an ecosystem. As such, this is the first evaluation of the uncertainty involved in the estimation of uptake and turnover using these experiments. Quantifying and managing such uncertainty is important in these experiments because of the limited amount of data involved, and because they measure phenomena that propagate across scales. Beyond accounting for sampling error, our method can handle three important sources of error or bias that were previously suboptimally handled. First, modeling the system as a whole ensures that the interdependence of parameter estimates among compartments becomes explicit, and thus the error in the estimates of nitrogen dynamics of a particular compartment is incorporated in the estimation of the compartments that consume it. In the past, this kind of error propagation has been ignored (Dodds et al., 2000). Second, it is now possible to model diet uncertainty at two levels: topological and quantitative. By topological uncertainty we refer to the uncertainty regarding the presence or absence of a particular trophic link. By modifying the topology of the transfer matrix $\mathbf{\Psi}$ (i.e. which elements $\psi_{i,j} \neq 0$), one can explicitly test different hypotheses regarding the trophic structure of the ecosystem using model selection techniques, and either select the best model or average across models using model averaging. We have illustrated how to do so using the DIC (Spiegelhalter et al., 2002), but other Bayesian techniques such as reversible jump MCMC (Green, 1995), or variable selection methods, can be implemented (see Tenan et al. (2014); Hooten and Hobbs (2015) for reviews on available methods). By quantitative uncertainty

we refer to the diet of organisms with more than one food source. Past models required the input of assumed proportions of each source. This is not necessary in our approach, and the proportion of each resource consumed (and its uncertainty) can be calculated as a derived parameter after the model fit (see Equation 29). Finally, our method offers a solution to the paradox of overenrichment, whereby consumer compartments appear more labelled than their sources (Dodds et al., 2014). It does so by allowing the partitioning of resource compartments into an active portion π_i that uptakes detectable marked nutrient during the time frame of the experiment, and a refractory one that doesn't (or does so at much larger time scales). Because this portion is an estimated parameter, its uncertainty is evaluated, which is an advantage over the *post hoc* multiplicative factor approach previously proposed (Dodds et al., 2014).

All the above mentioned sources of uncertainty get integrated to produce the uncertainty in the posterior distribution of the evaluated parameters. As exemplified by our case study, this uncertainty can sometimes be rather large, which is not surprising given the typically high dimensionality of these systems and the limited amount of data (due to the high cost of isotopic analysis and the need to minimize invasiveness). This highlights further the importance of measuring and reporting the uncertainty in the estimated parameters, in order to temper our statements on the results. One of the advantages of our Bayesian implementation is that it can incorporate prior knowledge to help reduce this uncertainty, a strategy increasingly used in ecological management (McCarthy and Masters, 2005). This can be in the form of supplementary experiments on specific organisms or published values on similar taxa and systems. Moreover, it is possible to evaluate the influence of prior information using prior sensitivity analysis, and therefore formally evaluate the contribution of our data to the increase (or decrease) of certainty in the studied parameters. Ultimately, our method can be used on simulated data prior to an experiment

in order to test out the power of alternative experimental designs regarding the dripping regime, and the sampling schedule of each compartment. In our opinion, this is one of the most powerful advantages of having a formal statistical framework available for isotope tracer experiments. While a full exploration of different designs is out of the scope of this article, two important aspects of the design that are important to parameter identifiability seem apparent to us. First, it is necessary to have good temporal resolution of samples where uptake of tracer changes slope significantly (e.g. at peak uptake). Second, if more than one nutrient is labeled (as is the case here with both forms of nitrogen), it is important that their labelling is not strongly positively correlated, if one is to distinguish differential uptake of each shource. In our example, the dynamics of nitrification ensure that, as $^{15}NH_4^+$ label decreases downstream, $^{15}NO_3^-$ increases, allowing us to tease apart $^{15}NH_4^+$ from $^{15}NO_3^-$ uptake.

Despite large uncertainties around some parameter values, we were able to identify some important expected differences in the functioning of the two study streams. For example, basal (and total fluxes) are higher in the open canopy stream (Figure 6A), as expected by the limiting effect of light in forested streams (Vannote et al., 1980). This result is consistent with previous analyses (Collins et al., 2016), and with other contemporary work in the same study sites that show an increase of chlorophyll a abundance with light (Kohler et al., 2012), and increased gross primary production (GPP) in the open canopy stream (Leduc et al. in revision). Our analysis also clearly shows a higher ratio of NO_3^- to NH_4^+ use by epilithon in the open canopy stream (Figure 6B). This is consistent with the fact that NH_4^+ is the preferred form of nitrogen to algae, and as light increases, the higher nutrient demand drives algae to use other sources of nitrogen, such as NO_3^- (Morris, 1974).

Our analysis also suggests potential biases in previous estimation methods that ap-

proximate post-drip ^{15}N turnover by fitting an exponential decay curve (Collins et al., 2016). Previous estimates show higher consumer turnover times than our statistical implementation, and consequently, higher uptake rates, too (in order to maintain the same observed ^{15}N concentration). This could be due to the increasing difficulty of detecting a clear exponential decrease in the isotopic ratio with increasing trophic level. The converse pattern is true for basal compartments: our approach estimates higher turnover times and higher uptake rates than Collins et al. (2016). This may be a consequence of our splitting of basal compartments in active and refractory portions. In Collins et al. (2016), primary consumers need to eat a larger quantity of their resource to get enough ^{15}N signal, while in our model, they need to eat a lower biomass of the active portion, which has higher ^{15}N concentration. Less consumption should result in lower turnover rates and higher turnover times. A full investigation of the potential biases of the different methods will require an intensive simulation approach.

Through our model selection exercise, we were also able to contrast some of the topological assumptions of Collins et al. (2016). While Collins et al. assumed that *Eudaniela* crabs consume comparable amounts of CBOM and FBOM, our model selection exercise shows clear evidence against the consumption of FBOM. On the other hand, while in Collins et al. we assume that *Argia* damselflies only consume *Tricorythodes* mayflies, we found evidence in favour of them also preying on *Petrophila* larvae. This illustrates the power and importance of being able to perform model selection on isotope tracer experiments. Against *a priori* expectations, some of the untested links appear very weak (e.g. consumption of *Petrophila* by *Argia*). The purpose of our model comparison was illustrative, and a thorough examination of all trophic links is out of the scope of our article, but we hope it is clear how this would be a straightforward exercise. We must caution, however, that the number of models increases exponentially with every link tested, and

one must be wary of the risks of data-dredging and overanalysis that come with testing too many models if there are no *a priori* reasons to test them all.

For all its advantages, from error propagation to the use of prior information, Bayesian models do have a main inconvenience: computing time. It took on average four hours of computation to fit a single model to one stream, using parallel computing of the four MCMC chains on an Intel (R) CoreTM i5 processor (4590 3.3GHz) and 8GB of RAM. Given that one of the strongest motivations to use this method is the need to statistically analyze the increasing number of large comparative studies (Mulholland et al., 2008; Norman et al., 2017; Tank et al., 2018), this is an important concern. However, faster computers and large clusters are likely to reduce these times quickly. It is also important to be aware of the method's limitations and simplifications. First, our model is based a linear Markov process, which means that all transfer rates are a constant proportion of resource abundance. Strictly speaking, this is not a realistic assumption, since algal uptake often follow a non linear function of nutrient availability, such as Michaelis-Menten dynamics (O'Brien, 1974), and consumers show saturating functional responses to prey abundance (Jeschke et al., 2002). However, this simplification, common to previous methods, is easily justified given the relatively short time-frame of isotope tracer addition experiments. This makes it unlikely that resource abundance will vary to the point that non-linearities cannot be approximated locally by linear functions. In fact, our methods assumes that the system is approximately at steady state, meaning that there are no major changes in the biomass of compartments during the period of the study. It is possible that this assumption won't hold for some longer experiments in highly productive environments, and future developments of the model may alleviate this assumption using time series of biomass data throughout the experiment.

We can think of other aspects that can be incorporated into this framework in the

future other than non-linear uptake and growth dynamics. For example, this model could incorporate the longitudinal dimension explicitly, as was done in Newbold et al. (1983). In that effort, the water column was treated as a dynamic compartment and included particle exchange between the bed and the water column (the latter being critical to fitting the dynamics of the net-spinning caddisfly). The present manuscript, by contrast, is not spatially explicit, replaces the water column dynamics with external forcing, and neglects particle suspension, transport and deposition. An explicit treatment of flow and longitudinal linkage would allow one to combine the temporal and spatial information of tracer distribution along the stream in order to increase the accuracy of our estimates of uptake, and turnover. This can be particularly powerful for understanding the dynamics of nutrient pools and basal compartments (e.g. nitrification), whose faster dynamics makes tracer differences most apparent along the spatial axis (Mulholland et al., 2000; Peterson et al., 2001). A second potential development is the incorporation of nutrient cycling in the form of excretion or decomposition. This would essentially involve a new set of parameters ρ_i denoting the recycling rate of compartment i, (i.e. the proportion of that compartment that returns to the NH_4^+ pool). These parameters would populate the first row of the transfer matrix $\mathbf{\Psi}$. In order for compartment-specific recycling rates to be identifiable, however, they would likely require the incorporation of priors (e.g. using supplementary excretion trials), and the incorporation of the spatial scale proposed above.

Another possible development would be the integration of generalized linear mixed models (GLMMs; (Bolker et al., 2009)) or other models that allow for covariates to affect uptake and turnover rates. This would be particularly powerful in comparative analyses across different experiments and sites, as it would improve our ability to explicitly test effects of a paticular variable of interest (e.g. light, temperature, or time) across streams or treatments.

In conclusion, we have presented a method that improves the statistical rigor and of tracer addition analyses. Our hope is that it will not only be of great use as it stands, but also provide a baseline template for further developments and improvements that extract the most information from such elegant experiments. Most importantly, our modelling approach allows statistical comparisons among systems and treatments, as well as formal testing of alternative hypotheses, expanding the utility of isotope tracer experiments in comparative and experimental settings.

Acknowledgments

We would like to thank DL DeAngelis, G García-Costoya, S De Bona, SP Gordon, S Lambert, AEG Lee, and K Sidhu for fruitful discussions and comments on the manuscript. T Heatherly, KL McNeill, and AOH Leduc helped with different aspects of the tracer addition experiment. DN Reznick provided logistic support, infrastructure, and intellectual feedback throughout the performance of the tracer experiment. Funding was provided by grants from the Academy of Finland (#295941) to ALS and a FIBR grant of the National Science Foundation (EF0623632) to ASF and SAT.

Appendix: Tracer drip, sampling and chemical analysis

Biomass sampling

Biomass of food web compartments and water chemistry in both streams were monitored in March 2010 before isotope tracer releases began and in May 2010 after sampling concluded. Each stream had three biomass sampling sites. We sampled one pool and one riffle at each of the six sampling sites for a total of 6 samples per stream. Total biomass was calculated assuming that 60% of the benthic area is composed by riffles.

We collected filtered water samples for soluble reactive phosphorus (SRP) and nitrate (NO_3^-) that were frozen and returned to the US for analysis. Nitrate samples were analyzed using a Dionex ICS-90 ion chromatography system with Chromeleon software (Dionex Corporation) and SRP samples were analyzed on a Pharmacia LKB Ultraspec III spectrophotometer (model 80-2097-62; Pharmacia Biotech) using a method developed by Murphy & Riley (1962). We analyzed ammonium (NH_4^+) water chemistry in the field using fluorometric methods with an Aquaflor handheld flurometer (Turner Designs, Sunnyvale, CA). Ammonium samples collected in brown opaque bottles and kept cold for up to six hours until they were reacted with orthophthaldiadehyde (OPA). Fluorescence was measured 2-3 hours after the OPA reagent was added. We created a standard curve with stream water samples to correct for matrix effects and converted fluorescence to NH_4^+ concentration (Taylor et al. 2007).

Because both streams contained many large rocks and bedrock that could not be removed from the stream and scrubbed, we sampled epilithon with modified Loeb samplers (Loeb 1981). Seven Loeb samples per sampling site were combined into a single sample for analysis. Epilithon samples were subsampled and filtered through glass fiber filters (What-

man GF/F; 0.7 µm pore size) to analyze chlorophyll-a and ash free dry mass (AFDM). Suspended organic matter (seston) was collected on Whatman GF/F filters in the field by filtering a known quantity of stream water, between 1 and 2 L depending on seston concentration. Fine benthic organic matter (FBOM) was sampled by sinking a plastic cylinder (bottom area = 530 cm^2) into an area of soft sediment, measuring the water depth in the cylinder, mixing the surface layer of organic matter into the water, and removing a known quantity of slurry from the cylinder. Coarse benthic organic matter (CBOM) was sampled by haphazardly selecting a location on the stream and removing all leaf litter and woody material in a 0.5 m wide transect that stretched across the width of the stream at the selected location. We dried epilithon AFDM, seston, FBOM and CBOM samples at 50°C until they reached a constant mass and recorded all biomasses. After recording the mass of epilithon AFDM filters, we ashed filters at 450°C for six hours and recorded the mass of the filter plus ash.

Invertebrates were sampled at the same transects as basal resource compartments using a Hess sampler with a 0.032 m^2 area and a 250 µm net. We preserved invertebrate samples in 90% ethanol and returned them to the US for processing and enumeration. Biomass was calculated using standard length-mass relationships (Benke et al. 1999, Baumgartner & Rothhaupt 2003, Sabo et al. 2002, Miyasaka et al. 2008, T. Heatherly, unpublished data).

^{15}N-ammonium addition

We added ^{15}N labeled ammonium (as dissolved $^{15}NH_4Cl$) to both study reaches: canopy thinned (UL), and natural canopy (LL). We added the isotope using a continuous drip with an injection rate of 10 $mL.min^{-1}$ over a 10-day period from March 7th to 16th 2010. The injections increased the δ^{15}N of dissolved ammonium to approximately 20,000‰.

The target enrichment was not intended to fertilize the system, and the concentration of ^{15}N added was <5% of ambient NH_4^+. We also added rhodamine fluorescent dye as a conservative tracer throughout the course of the isotope release, which we used to correct for dilution along the study reach.

Isotope sampling and analysis

We sampled food web compartments to track the fate of the isotope tracers at three stations downstream of each point of isotope release (approximately 15, 30 and 60m downstream depending on the reach). Samples were collected on three days during the 10-day isotope release (Days 3, 7 and 10), and on five days during the month following the isotope release (Days 13, 17, 20, 30 and 40). Sampled food web compartments included: water chemistry ($^{15}NO_3^-$ and $^{15}NH_4^+$), epilithon, FBOM (sampled from the sediment surface via suction), CBOM, seston, and eight common invertebrate taxa representing all functional feeding groups (predators, grazers, collector-gatherers, collector-filterers and shredders). Invertebrate taxa selected were sufficiently large-bodied and abundant that they could be collected by hand with minimal disturbance to the streambed. Many of the invertebrate taxa we collected (*Eudaniela*, *Euthyplocia*, *Psephenus*, *Leptonema*, *Tricorythodes* and *Argia*) are among the dominant taxa in both streams, but two of our sampled invertebrate groups, *Petrophila sp.* and *Phylloicus sp.*, were not among the most abundant invertebrate taxa but represented functional feeding groups (scraper and shredder, respectively) distinct from those dominant in the streams. We were unable to collect some small-bodied but abundant taxa (e.g., chironomids) because we could not collect enough individuals for isotope sample analysis without causing major disturbance to the streambed. We also collected background samples from each compartment to correct for background isotopic values. Background samples were collected either prior to the start of the experiment or

from upstream of the control reach tracer addition point.

We dried all samples at 50°C and conducted isotopic analyses at the University of Georgia isotope analysis facility. Basal resource sampling protocols were the same as the biomass sampling techniques, but for invertebrates, we hand-picked individuals by turning over rocks and sorting through organic matter in plastic trays to minimize disturbance and ensure that sufficient numbers of each taxon were collected for isotopic analysis. We also measured water column ^{15}N, which we measured with a filter pack diffusion technique (Sigman et al. 1997, Holmes et al. 1998). Specifically, we collected 900 mL of water in 1 L plastic cubitainers for $^{15}NH_4^+$ samples and added a 60 µg spike of N as NH_4^+ to increase N mass to a level that is detectable by a mass spectrometer. We collected 500 mL of water for $^{15}NO_3^-$ samples and transferred samples in 250 mL Nalgene bottles after boiling to reduce volume to approximately 100 mL. Ammonium from all samples was allowed to diffuse onto a 1.0 cm Whatman GF/D (2.7 µm pore size) filter sealed in Teflon tape for at least three weeks before filters were harvested and dried at 50°C.

References

Ainsworth, C. H., I. C. Kaplan, P. S. Levin, and M. Mangel. 2010. A statistical approach for estimating fish diet compositions from multiple data sources: Gulf of California case study. Ecological Applications 20:2188–2202.

Ball, R. C., and F. F. Hooper. Translocation of phosphorus in a trout stream ecosystem. 1963.

Banašek-Richter, C., M.-F. Cattin, and L.-F. Bersier. 2004. Sampling effects and the robustness of quantitative and qualitative food-web descriptors. Journal of Theoretical Biology 226:23–32.

Berlow, E. L., A.-M. Neutel, J. E. Cohen, P. C. De Ruiter, B. Ebenman, M. Emmerson, J. W. Fox, V. A. A. Jansen, J. Iwan Jones, G. D. Kokkoris, D. O. Logofet, A. J. McKane, J. M. Montoya, and O. Petchey. 2004. Interaction strengths in food webs: issues and opportunities. Journal of Animal Ecology 73:585–598.

Boecklen, W. J., C. T. Yarnes, B. A. Cook, and A. C. James. 2011. On the Use of Stable Isotopes in Trophic Ecology. Annual Review of Ecology, Evolution, and Systematics 42:411–440.

Bolker, B. M., M. E. Brooks, C. J. Clark, S. W. Geange, J. R. Poulsen, M. H. H. Stevens, and J.-S. S. White. 2009. Generalized linear mixed models: a practical guide for ecology and evolution. Trends in Ecology & Evolution 24:127–135.

Bond, A. L., and A. W. Diamond. 2011. Recent Bayesian stable-isotope mixing models are highly sensitive to variation in discrimination factors. Ecological Applications 21:1017–1023.

Carpenter, B., A. Gelman, M. D. Hoffman, D. Lee, B. Goodrich, M. Betancourt, M. Brubaker, J. Guo, P. Li, and A. Riddell. 2017. *Stan* : A Probabilistic Programming Language. Journal of Statistical Software 76.

Carpenter, S. R., J. J. Cole, M. L. Pace, M. Van de Bogert, D. L. Bade, D. Bastviken, C. M. Gille, J. R. Hodgson, J. F. Kitchell, and E. S. Kritzberg. 2005. Ecosystem subsidies: Terrestrial support of aquatic food webs from 13c addition to contrasting lakes. Ecology 86:2737–2750.

Cole, J. J., S. R. Carpenter, J. F. Kitchell, and M. L. Pace. 2002. Pathways of organic carbon utilization in small lakes: Results from a whole-lake 13c addition and coupled model. Limnology and Oceanography 47:1664–1675.

Collins, S. M., S. A. Thomas, T. Heatherly, K. L. MacNeill, A. O. H. C. Leduc, A. López-Sepulcre, B. A. Lamphere, R. W. El-Sabaawi, D. N. Reznick, C. M. Pringle, and A. S. Flecker. 2016. Fish introductions and light modulate food web fluxes in tropical streams: a whole-ecosystem experimental approach. Ecology 97:3154–3166.

Dodds, W. K., S. M. Collins, S. K. Hamilton, J. L. Tank, S. Johnson, J. R. Webster, K. S. Simon, M. R. Whiles, H. M. Rantala, W. H. McDowell, S. D. Peterson, T. Riis, C. L. Crenshaw, S. A. Thomas, P. B. Kristensen, B. M. Cheever, A. S. Flecker, N. A. Griffiths, T. Crowl, E. J. Rosi-Marshall, R. El-Sabaawi, and E. Martí. 2014. You are not always what we think you eat: selective assimilation across multiple whole-stream isotopic tracer studies. Ecology 95:2757–2767.

Dodds, W. K., M. A. Evans-White, N. M. Gerlanc, L. Gray, D. A. Gudder, M. J. Kemp, A. L. López, D. Stagliano, E. A. Strauss, J. L. Tank, M. R. Whiles, and W. M. Wollheim. 2000. Quantification of the Nitrogen Cycle in a Prairie Stream. Ecosystems 3:574–589.

Elton, C. S. 1927. *Animal ecology*. University of Chicago Press, Chicago IL.

Elwood, J. W., and D. J. Nelson. 1972. Periphyton production and grazing rates in a stream measured with a 32 p material balance method. Oikos pages 295–303.

Gelman, A., J. Carlin, H. Stern, and D. Rubin. 2003. *Bayesian Data Analysis, Second Edition*. Chapman & Hall/CRC Texts in Statistical Science. Taylor & Francis.

Geman, S., and D. Geman. 1984. Stochastic Relaxation, Gibbs Distributions, and the Bayesian Restoration of Images. IEEE Transactions on Pattern Analysis and Machine Intelligence PAMI 6:721–741.

Goodale, C. L., G. Fredriksen, M. S. Weiss, C. K. McCalley, J. P. Sparks, and S. A. Thomas. 2015. Soil processes drive seasonal variation in retention of 15n tracers in a deciduous forest catchment. Ecology 96:2653–2668.

Green, P. J. 1995. Reversible jump Markov chain Monte Carlo computation and Bayesian model determination. Biometrika 82:711–732.

Hooten, M. B., and N. T. Hobbs. 2015. A guide to Bayesian model selection for ecologists. Ecological Monographs 85:3–28.

Hutchinson, G. E., and V. T. Bowen. 1950. Limnological studies in connecticut. ix. a quantitative radiochemical study of the phosphorus cycle in linsley pond. Ecology 31:194–203.

Iosifescu, M. 1980. *Finite Markov processes and their applications*. Wiley, Chichester. OCLC: 848156627.

Jardine, T. D., W. L. Hadwen, S. K. Hamilton, S. Hladyz, S. M. Mitrovic, K. A. Kidd, W. Y. Tsoi, M. Spears, D. P. Westhorpe, V. M. Fry, F. Sheldon, and S. E. Bunn. 2014.

Understanding and Overcoming Baseline Isotopic Variability in Running Waters. River Research and Applications 30:155–165.

Jeschke, J. M., M. Kopp, and R. Tollrian. 2002. Predator Functional Responses: Discriminating Between Handling and Digesting Prey. Ecological Monographs 72:95–112.

King, R. 2014. Statistical Ecology. Annual Review of Statistics and Its Application 1:401–426.

Kling, G. W. 1994. Ecosystem-Scale Experiments. Pages 91–120 *in* Environmental Chemistry of Lakes and Reservoirs, volume 237 of *Advances in Chemistry*. American Chemical Society.

Kohler, T. J., T. N. Heatherly, R. W. El-Sabaawi, E. Zandonà, M. C. Marshall, A. S. Flecker, C. M. Pringle, D. N. Reznick, and S. A. Thomas. 2012. Flow, nutrients, and light availability influence Neotropical epilithon biomass and stoichiometry. Freshwater Science 31:1019–1034.

Kulmatiski, A., K. H. Beard, R. J. T. Verweij, and E. C. February. 2010. A depth-controlled tracer technique measures vertical, horizontal and temporal patterns of water use by trees and grasses in a subtropical savanna. New Phytologist 188:199–209.

Ledger, M. E., L. E. Brown, F. K. Edwards, A. M. Milner, and G. Woodward. 2013. Drought alters the structure and functioning of complex food webs. Nature Climate Change 3:223–227.

Lima, M., N. C. Stenseth, and F. M. Jaksic. 2002. Food web structure and climate effects on the dynamics of small mammals and owls in semi-arid Chile. Ecology Letters 5:273–284.

Link, W. A., and R. J. Barker. 2010. *Bayesian Inference: with ecological applications*.

Lopez-Sepulcre, A., M. Bruneaux, S. M. Collins, R. El-Sabaawi, A. S. Flecker, and S. A. Thomas. 2020. Data from: A new method to reconstruct quantitative food webs and nutrient flows from isotope tracer addition experiments. American Naturalist, Dryad, Dataset, https://doi.org/10.5061/dryad.8sf7m0chx

McCarthy, M. A., and P. Masters. 2005. Profiting from prior information in Bayesian analyses of ecological data. Journal of Applied Ecology 42:1012–1019.

Middelburg, J. J., C. Barranguet, H. T. S. Boschker, P. M. J. Herman, T. Moens, and C. H. R. Heip. 2000. The fate of intertidal microphytobenthos carbon: An in situ 13c-labeling study. Limnology and Oceanography 45:1224–1234.

Morris, I. 1974. Nitrogen assimilation and protein synthesis. Algal Physiology and Biochemistry 10.

Mulholland, P. J., J. L. Tank, D. M. Sanzone, W. M. Wollheim, B. J. Peterson, J. R. Webster, and J. L. Meyer. 2000. Nitrogen Cycling in a Forest Stream Determined by a 15n Tracer Addition. Ecological Monographs 70:471–493.

Mulholland, P. J., A. M. Helton, G. C. Poole, R. O. Hall, S. K. Hamilton, B. J. Peterson, J. L. Tank, L. R. Ashkenas, L. W. Cooper, C. N. Dahm, W. K. Dodds, S. E. G. Findlay, S. V. Gregory, N. B. Grimm, S. L. Johnson, W. H. McDowell, J. L. Meyer, H. M. Valett, J. R. Webster, C. P. Arango, J. J. Beaulieu, M. J. Bernot, A. J. Burgin, C. L. Crenshaw, L. T. Johnson, B. R. Niederlehner, J. M. O'Brien, J. D. Potter, R. W. Sheibley, D. J. Sobota, and S. M. Thomas. 2008. Stream denitrification across biomes and its response to anthropogenic nitrate loading. Nature 452:202–205.

Mulholland, R. J., and M. S. Keener. 1974. Analysis of linear compartment models for ecosystems. Journal of theoretical biology 44:105–116.

Newbold, J. D., J. W. Elwood, R. V. O'Neill, and A. L. Sheldon. 1983. Phosphorus Dynamics in a Woodland Stream Ecosystem: A Study of Nutrient Spiralling. Ecology 64:1249–1265.

Norman, B. C., M. R. Whiles, S. M. Collins, A. S. Flecker, S. K. Hamilton, S. L. Johnson, E. J. Rosi, L. R. Ashkenas, W. B. Bowden, C. L. Crenshaw, T. Crowl, W. K. Dodds, R. O. Hall, R. El-Sabaawi, N. A. Griffiths, E. Marti, W. H. McDowell, S. D. Peterson, H. M. Rantala, T. Riis, K. S. Simon, J. L. Tank, S. A. Thomas, D. v. Schiller, and J. R. Webster. 2017. Drivers of nitrogen transfer in stream food webs across continents. Ecology 98:3044–3055.

O'Brien, W. J. 1974. The Dynamics of Nutrient Limitation of Phytoplankton Algae: A Model Reconsidered. Ecology 55:135–141.

Pace, M. L., J. J. Cole, S. R. Carpenter, J. F. Kitchell, J. R. Hodgson, M. C. Van de Bogert, D. L. Bade, E. S. Kritzberg, and D. Bastviken. 2004. Whole-lake carbon-13 additions reveal terrestrial support of aquatic food webs. Nature 427:240.

Paine, R. T. 1980. Food Webs: Linkage, Interaction Strength and Community Infrastructure. Journal of Animal Ecology 49:667–685.

Patten, B. C., and M. Witkamp. 1967. Systems analysis of 134cesium kinetics in terrestrial microcosms. Ecology 48:813–824.

Peterson, B. J., and B. Fry. 1987. Stable Isotopes in Ecosystem Studies. Annual Review of Ecology and Systematics 18:293–320.

Peterson, B. J., W. M. Wollheim, P. J. Mulholland, J. R. Webster, J. L. Meyer, J. L. Tank, E. Martí, W. B. Bowden, H. M. Valett, A. E. Hershey, W. H. McDowell, W. K. Dodds,

S. K. Hamilton, S. Gregory, and D. D. Morrall. 2001. Control of Nitrogen Export from Watersheds by Headwater Streams. Science 292:86–90.

Post, D. M. 2002. Using Stable Isotopes to Estimate Trophic Position: Models, Methods, and Assumptions. Ecology 83:703–718.

R Core Team. 2019. *R: A Language and Environment for Statistical Computing*. R Foundation for Statistical Computing, Vienna, Austria.

Rigler, F. H. 1956. A tracer study of the phosphorus cycle in lake water. Ecology 37:550–562.

Rooney, N., and K. S. McCann. 2012. Integrating food web diversity, structure and stability. Trends in Ecology & Evolution 27:40–46.

Roslin, T., and S. Majaneva. 2016. The use of DNA barcodes in food web construction-terrestrial and aquatic ecologists unite! Genome 59:603–628.

Spiegelhalter, D. J., N. G. Best, B. P. Carlin, and A. Van Der Linde. 2002. Bayesian measures of model complexity and fit. Journal of the royal statistical society: Series b (statistical methodology) 64:583–639.

Stan Development Team. 2019. RStan: the R interface to Stan. R package version 2.19.2.

Tank, J. L., E. Martí, T. Riis, D. v. Schiller, A. J. Reisinger, W. K. Dodds, M. R. Whiles, L. R. Ashkenas, W. B. Bowden, S. M. Collins, C. L. Crenshaw, T. A. Crowl, N. A. Griffiths, N. B. Grimm, S. K. Hamilton, S. L. Johnson, W. H. McDowell, B. M. Norman, E. J. Rosi, K. S. Simon, S. A. Thomas, and J. R. Webster. 2018. Partitioning assimilatory nitrogen uptake in streams: an analysis of stable isotope tracer additions across continents. Ecological Monographs 88:120–138.

Tenan, S., R. B. O'Hara, I. Hendriks, and G. Tavecchia. 2014. Bayesian model selection: The steepest mountain to climb. Ecological Modelling 283:62–69.

Travis, J., D. Reznick, R. D. Bassar, A. López-Sepulcre, R. H. J. Ferriere, and T. Coulson. 2014. Do eco-evo feedbacks help us understand nature? Answers from studies of the Trinidadian guppy. Advances in Ecological Research 50:1–40.

Vannote, R. L., G. W. Minshall, K. W. Cummins, J. R. Sedell, and C. E. Cushing. 1980. The River Continuum Concept. Canadian Journal of Fisheries and Aquatic Sciences 37:130–137.

Whiles, M. R., R. O. Hall, W. K. Dodds, P. Verburg, A. D. Huryn, C. M. Pringle, K. R. Lips, S. S. Kilham, C. Colón-Gaud, A. T. Rugenski, S. Peterson, and S. Connelly. 2013. Disease-Driven Amphibian Declines Alter Ecosystem Processes in a Tropical Stream. Ecosystems 16:146–157.

Whittaker, R. H. 1961. Experiments with radiophosphorus tracer in aquarium microcosms. Ecological monographs 31:157–188.

Zucchini, W., and I. L. MacDonald. 2009. *Hidden Markov models for time series: an introduction using R.* OCLC: 401461291.

Tables

Table 1: Notation.

Parameter	Description	Domain	Units
Observed variables			
C	Number of ecosystem compartments	$\mathbb{N}$	-
$\mathcal{I}$	Set of dissolved inorganic nutrient compartments	-	-
$\mathcal{B}$	Set of basal resources uptaking dissolved nutrients	-	-
$x_{\text{obs},i}^{(s,t)}$	Biomass of compartment i at sampling point s and time t	$(0,\infty)$	mgN/m^2
$z_{\text{obs},i}^{(s,t)}$	Proportion of marked isotope in compartment i at s and time t	$(0,1)$	1
SD_i	Coefficient of variation of compartment biomasses x_i	$(0,1)$	1
State variables			
$\mathbf{x}^{(s,t)}$	$C\times 1$ vector of elements $x_i^{(s,t)}$ = nutrient mass in compartment i at sampling point s and time t	$(0,\infty)$	mgN/m^2
$\mathbf{n}^{(s,t)}$	$C\times 1$ vector of elements $n_i^{(s,t)}$ = unmarked nutrient mass in compartment i at sampling point s and time t	$(0,\infty)$	mgN/m^2
$\mathbf{m}^{(s,t)}$	$C\times 1$ vector of elements $m_i^{(s,t)}$ = marked nutrient mass in compartment i at sampling point s and time t	$(0,\infty)$	mgN/m^2
$\mathbf{z}^{(s,t)}$	$C\times 1$ vector of elements $z_i^{(s,t)}$ = proportion of heavy isotope for compartment i at sampling point s and time t	$(0,1)$	1
$\mathbf{y_n}^{(s,t)}$	$C\times 1$ vector of elements $y_{n,i}^{(s)}$ = external input of unmarked nutrient into i at sampling point s and time t	$(0,\infty)$	mgN/m^2
$\mathbf{y_m}^{(s,t)}$	$C\times 1$ vector of elements $y_{m,i}^{(s)}$ = external input of marked nutrient into i at sampling point s and time t	$(0,\infty)$	mgN/m^2
Estimated parameters			
$\mathbf{\Psi_h}$	Transition matrix of elements $\psi_{i,j}$ = rate of nutrient transition between compartments j and i under model $\mathbf{h}$	$(0,1)$	day^{-1}
$\upsilon_{i,j}$	Uptake rate from compartment j to i	$(0,1)$	day^{-1}
λ_i	Loss rate of compartment i	$(0,1)$	day^{-1}
k_i	Turnover rate of compartment i	$(0,1)$	day^{-1}
π_i	Active (i.e. non refractory) portion of compartment i	$(0,1)$	1
η	Coefficient of variation of the isotopic proportions $z_{i,j}$	$(0,1)$	1
Derived parameters			
$\hat{X}_i$	Expected steady-state biomass of compartment i	$(0,\infty)$	mgN/m^2
T_i	Turnover time of the active portion of compartment i	$(0,\infty)$	day
T_i'	Apparent turnover time of compartment i	$(0,\infty)$	day
$F_{i,j}$	Flux between compartment j and i	$(0,\infty)$	mgN/m^2 day
F_T	Total nutrient flux	$(0,\infty)$	mgN/m^2 day
$P_{i,j}^U$	Proportion of compartment i's total uptake coming from j	$(0,1)$	1
$P_{i,j}^K$	Proportionof compartment j's turnover due to uptake by i	$(0,1)$	1

Table 2: Comparison of alternative models of food web structure regarding *Argia* and *Eudaniela* diets.

Model	Trophic link			# param.	DIC	ΔDIC	w_{DIC}
	Petrophila → *Argia*	*Psephenus* → *Argia*	FBOM → *Eudaniella*				
$\mathbf{\Psi}_{100}$	Yes	No	No	68	-2844.8	0	0.757
$\mathbf{\Psi}_{110}$	Yes	Yes	No	70	-2841.5	3.3	0.146
$\mathbf{\Psi}_{000}$	No	No	No	66	-2839.3	5.4	0.05
$\mathbf{\Psi}_{010}$	No	Yes	No	68	-2839.1	5.6	0.046
$\mathbf{\Psi}_{111}$	Yes	Yes	Yes	72	-2830	14.8	0
$\mathbf{\Psi}_{011}$	No	Yes	Yes	70	-2828.2	16.6	0
$\mathbf{\Psi}_{101}$	Yes	No	Yes	70	-2823.9	20.8	0
$\mathbf{\Psi}_{001}$	No	No	Yes	68	-2810.5	34.2	0

Equation boxes

$$\mathbf{\Psi_{111}} = \begin{bmatrix} \psi_{1,1} & 0 & 0 & 0 & 0 & 0 & 0 & 0 & 0 & 0 & 0 & 0 & 0 & 0 \\ 0 & \psi_{2,2} & 0 & 0 & 0 & 0 & 0 & 0 & 0 & 0 & 0 & 0 & 0 & 0 \\ \upsilon_{epi,NH4} & \upsilon_{epi,NO3} & -\lambda_{epi} & 0 & 0 & 0 & 0 & 0 & 0 & 0 & 0 & 0 & 0 & 0 \\ \upsilon_{ses,NH4} & \upsilon_{ses,NO3} & 0 & -\lambda_{ses} & 0 & 0 & 0 & 0 & 0 & 0 & 0 & 0 & 0 & 0 \\ \upsilon_{FBOM,NH4} & \upsilon_{FBOM,NO3} & 0 & 0 & -\lambda_{FBOM} & 0 & 0 & 0 & 0 & 0 & 0 & 0 & 0 & 0 \\ \upsilon_{CBOM,NH4} & \upsilon_{CBOM,NO3} & 0 & 0 & 0 & -\lambda_{CBOM} & 0 & 0 & 0 & 0 & 0 & 0 & 0 & 0 \\ 0 & 0 & \upsilon_{pet,NO3} & 0 & 0 & 0 & -\lambda_{pet} & 0 & 0 & 0 & 0 & 0 & 0 & 0 \\ 0 & 0 & \upsilon_{pse,NO3} & 0 & 0 & 0 & 0 & -\lambda_{pse} & 0 & 0 & 0 & 0 & 0 & 0 \\ 0 & 0 & 0 & \upsilon_{lep,ses} & 0 & 0 & 0 & 0 & -\lambda_{lep} & 0 & 0 & 0 & 0 & 0 \\ 0 & 0 & 0 & 0 & \upsilon_{tri,FBOM} & 0 & 0 & 0 & 0 & -\lambda_{tri} & 0 & 0 & 0 & 0 \\ 0 & 0 & 0 & 0 & 0 & \upsilon_{eud,CBOM} & 0 & 0 & 0 & 0 & -\lambda_{eud} & 0 & 0 & 0 \\ 0 & 0 & 0 & 0 & 0 & \upsilon_{phy,CBOM} & 0 & 0 & 0 & 0 & 0 & -\lambda_{phy} & 0 & 0 \\ 0 & 0 & 0 & 0 & 0 & 0 & 0 & 0 & \upsilon_{arg,lep} & \upsilon_{arg,tri} & 0 & 0 & -\lambda_{arg} & 0 \\ 0 & 0 & 0 & 0 & 0 & 0 & 0 & 0 & 0 & 0 & 0 & \upsilon_{eut,phy} & 0 & -\lambda_{eut} \end{bmatrix}$$

Box 1: Transition matrix describing the food web structure assumed by Collins et al. (2016).

Figures legends

Figure 1: Schematic example/representation of a Hidden Markov Model and food-web matrix.

Figure 2: Model fit for comparing data with credible and prediction envelopes. Solid dots are observed data; dark grey envelopes are 95% credible intervals; and light grey envelopes are 95% prediction intervals. Only data for the first transect of each stream is shown here. Profiles for all three transects can be found in the Supplementary Material (Figure S1).

Figure 3: Estimates of uptake fluxes and turnover times of all compartments for Lower La Laja (solid symbols), and Upper La Laja (open symbols). Circles and error bars represent our estimates and 95% credible intervals. Triangles represent the estimates made by Collins et al. (2016). Turnover was not estimated for *Argia* nor *Euthyplocia* in Collins et al. (2016). Note that the axis scale is logarithmic.

Figure 4: Quantitative food web reconstruction of the two streams. Compartments are represented by boxes and fluxes between them, by filled curved lines connecting them. The white box area represents the active portion of the compartment π_i, while the grey hatched area on the basal compartments represents the non-active (refractory) proportion $(1-\pi_i)$. Curve thickness is proportional to the flux rate calculated following Equation 23. The height of all non-nutrient compartment boxes is therefore proportional to the total uptake of N by that compartment. Box widths of non-nutrient compartments are proportional to the compartment's turnover time, with the width of the white area representing the turnover time of the active component, and the total width, the overall turnover time. The area of the box is therefore proportional to the compartment's biomass under the steady-state assumption (as per Equation 25). Note that the consumer fluxes (right) and biomasses have been magnified by 10x in order to visualize differences between streams.

Figure 5: Distribution of total NH_4^+ and NO_3^- uptake among the three main basal compartments. Grey areas represent 95% credible bounds. The dashed isoline indicates equal uptake of NH_4^+ and NO_3^-, with estimates above it indicating a dominance of NO_3^- uptake over NH_4^+ . Estimated values can be seen in Table S3. Seston uptake is not visible because it is very close to zero and has small credible bounds.

Figure 6: Statistical comparisons of derived parameters between streams. Each panel is composed of two plots: an upper plot with the estimate (and 95% credible intervals) for both streams side by side, and a lower plot with the distribution of the difference (or ratio), and its 95% credible intervals. Each panel corresponds to a derived parameter: (A) Total N flux F_T, (B) ratio of NO_3^- to NH_4^+ uptake by epilithon $R_{\text{epi,NO3}}$, (C) proportion of *Petrophila* N in the diet of *Argia* $P^K_{\text{arg,pet}}$, and (D) contribution of *Eudaniela* consumption to CBOM turnover $P^U_{\text{eud,CBOM}}$.

Figure 1

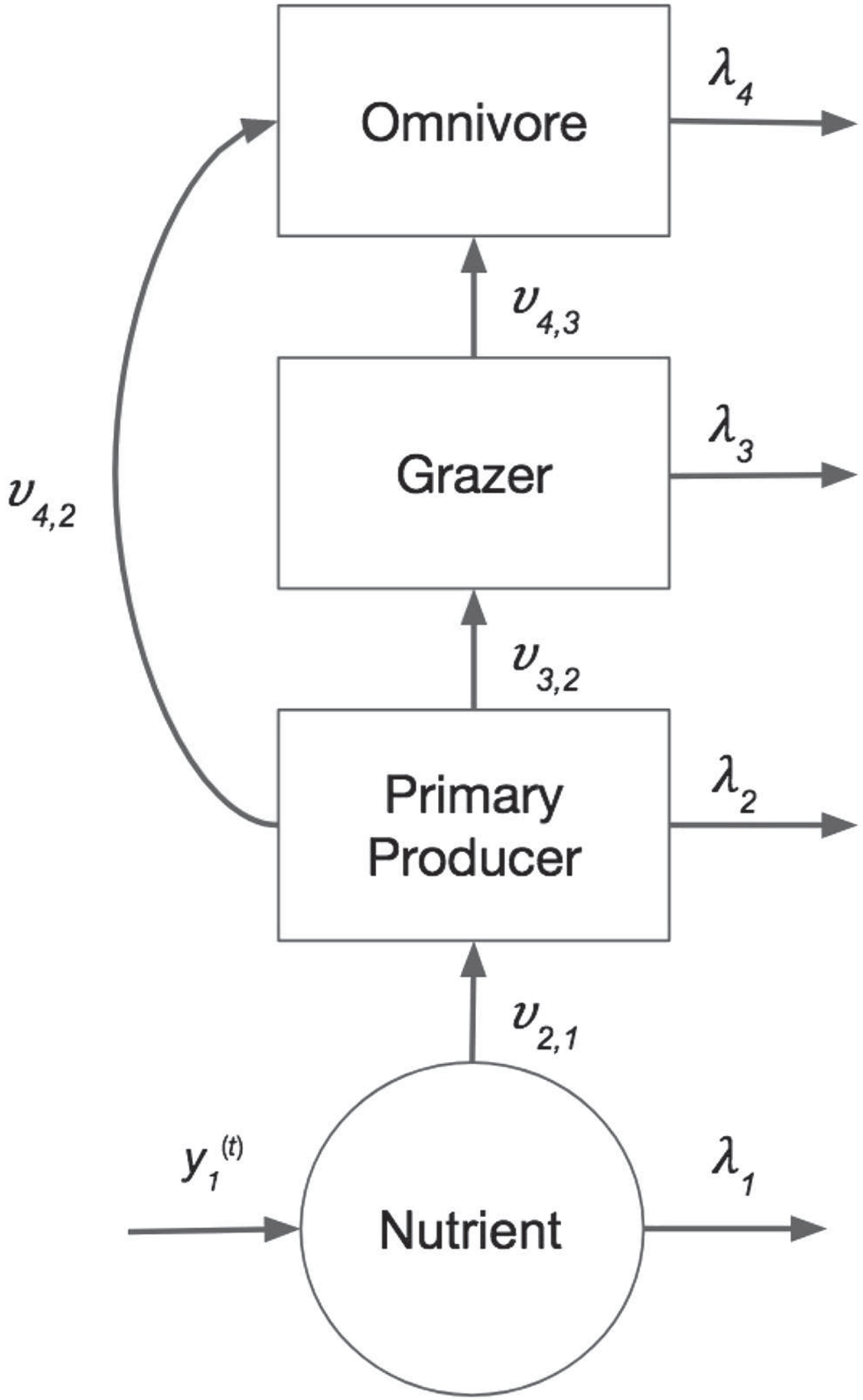
Omnivore
Grazer
Primary Producer
Nutrient
λ_4
λ_3
λ_2
λ_1
$\upsilon_{4,3}$
$\upsilon_{3,2}$
$\upsilon_{2,1}$
$\upsilon_{4,2}$
$y_1^{(t)}$

Figure 2

Open canopy (UL)
Closed canopy (LL)
Leptonema
Phylloicus
Eudaniela
Petrophila
Psephenus
Tricorythodes
Argia
Euthyplocia
Sestón
CBOM
Epilithon
FBOM
δ15N
Time (days)
0
10
20
30
40
500
1000
1500
2000
2500
3000

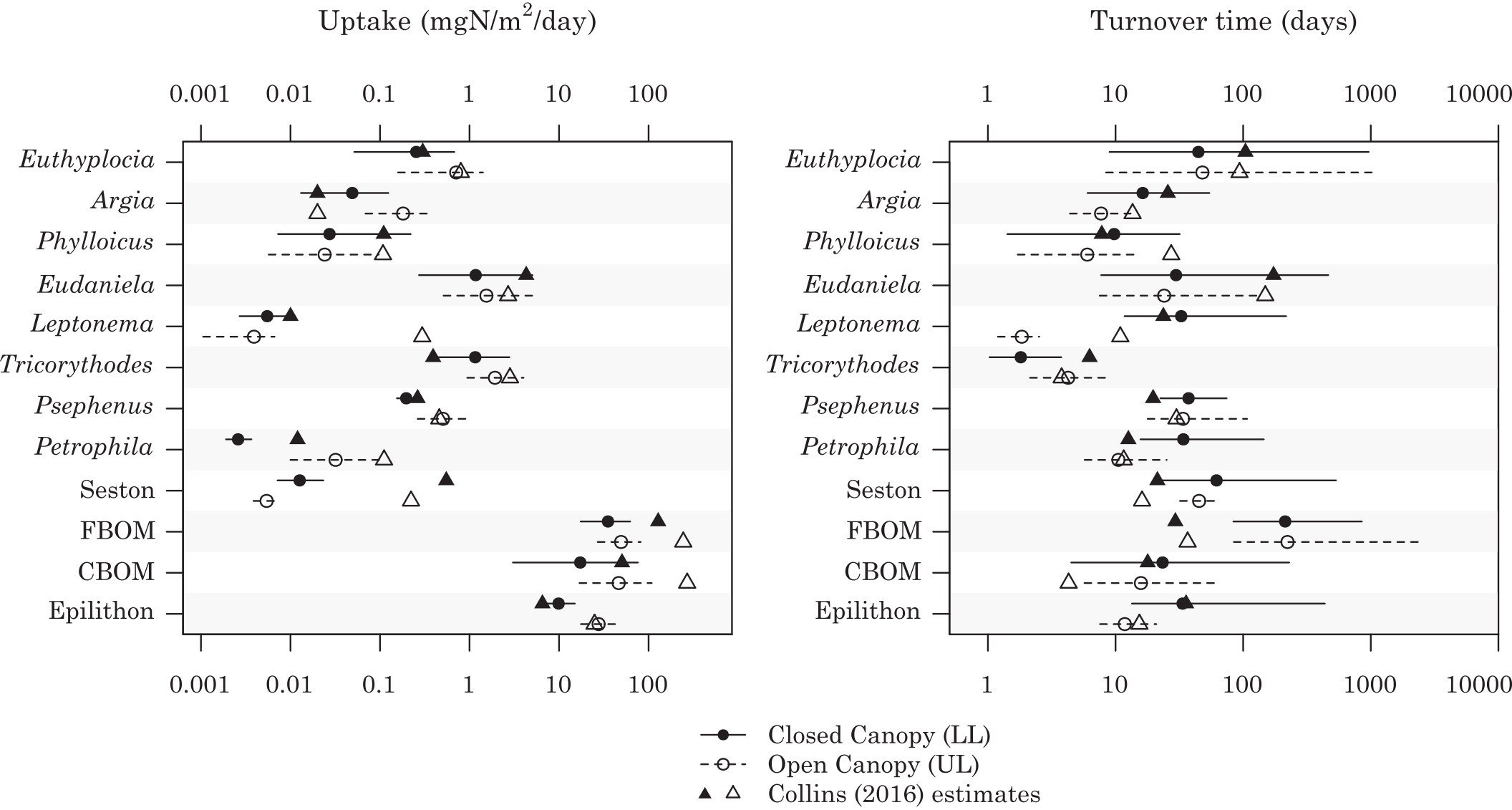
Uptake (mgN/m^2/day)
0.001
0.01
0.1
1
10
100
Turnover time (days)
1
10
100
1000
10000
Euthyplocia
Argia
Phylloicus
Eudaniela
Leptonema
Tricorythodes
Psephenus
Petrophila
Seston
FBOM
CBOM
Epilithon
Closed Canopy (LL)
Open Canopy (UL)
Collins (2016) estimates

Figure 4

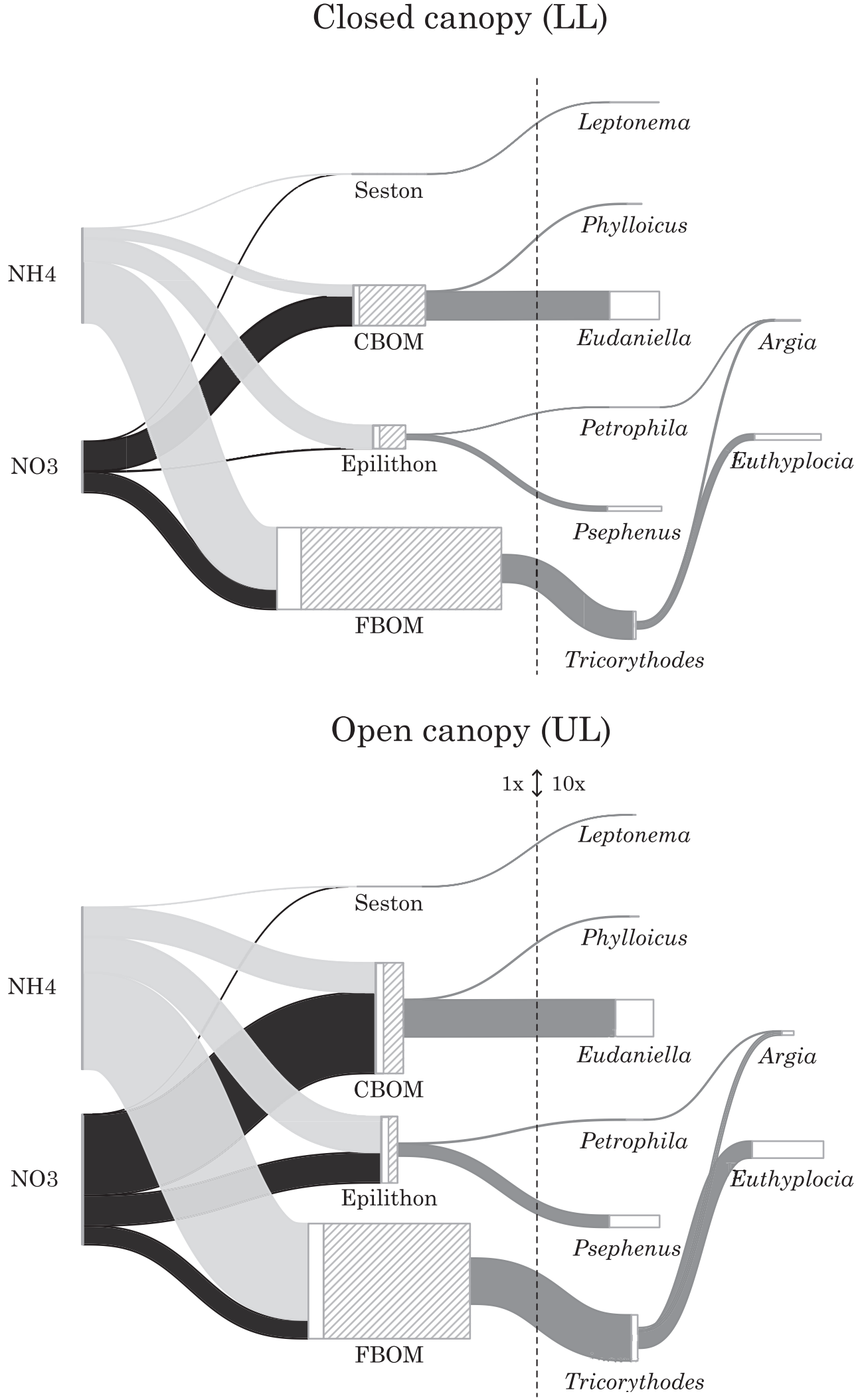
Closed canopy (LL)
NH4
NO3
Seston
CBOM
Epilithon
FBOM
Leptonema
Phylloicus
Eudaniella
Petrophila
Psephenus
Tricorythodes
Argia
Euthyplocia
Open canopy (UL)
1x
10x
NH4
NO3
Seston
CBOM
Epilithon
FBOM
Leptonema
Phylloicus
Eudaniella
Petrophila
Psephenus
Tricorythodes
Argia
Euthyplocia

Figure 5

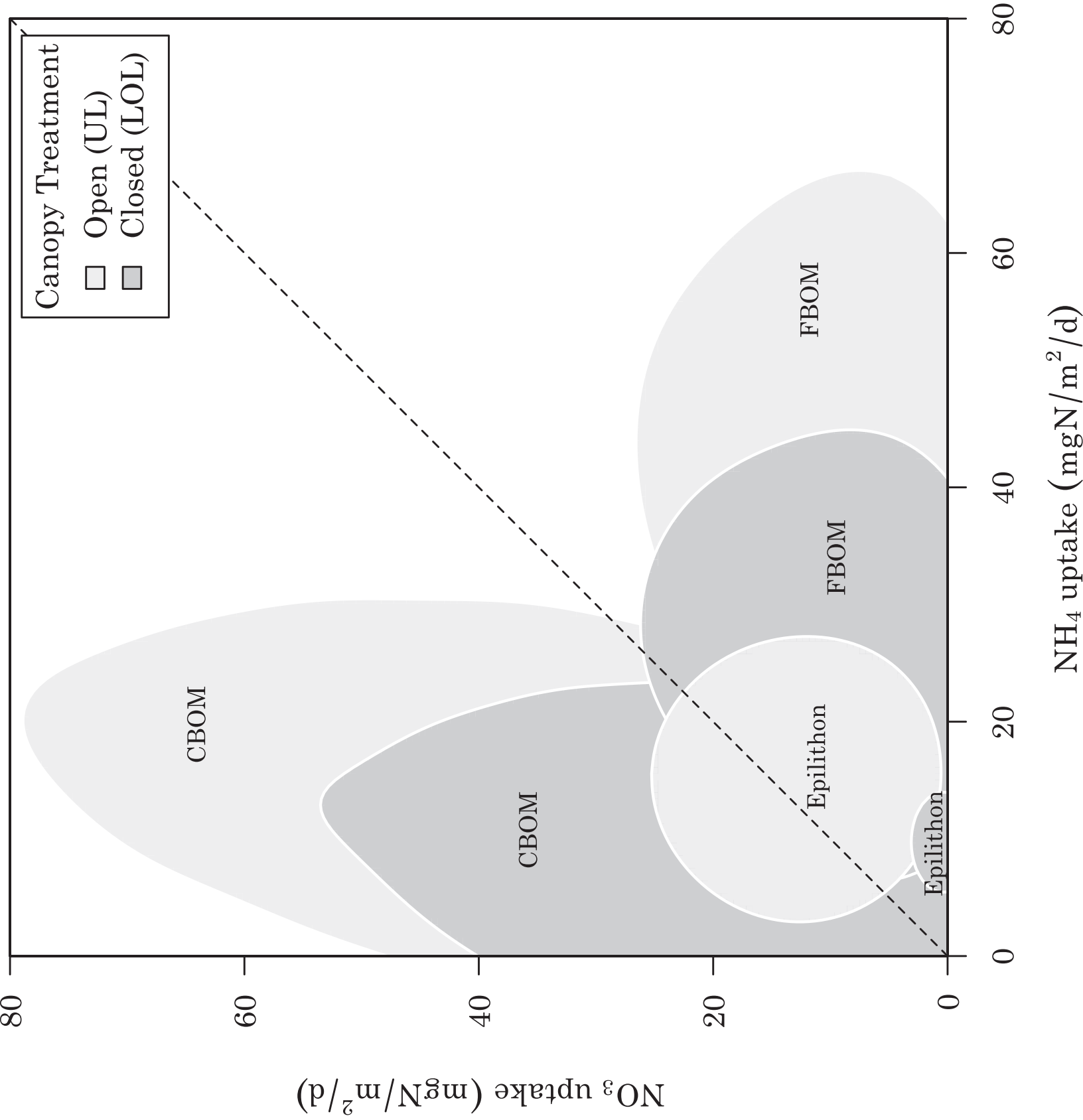
Canopy Treatment
Open (UL)
Closed (LOL)
CBOM
CBOM
Epilithon
Epilithon
FBOM
FBOM
0
20
40
60
80
0
20
40
60
80
NO3 uptake (mgN/m2/d)
NH4 uptake (mgN/m2/d)

Figure 6

(A)
(B)
(C)
(D)
LL
UL
$F_T(mgN/m^2/day)$
$R_{epi,NO3}$
$P^K_{eud,CBOM}$
$P^U_{arg,pet}$
$(F_T)^{UL} - (F_T)^{LL}$
$(R_{epi,NO3})^{UL}/(R_{epi,NO3})^{LL}$
$\text{logit}((P^K_{eud,CBOM})^{UL}) - \text{logit}((P^K_{eud,CBOM})^{LL})$
$\text{logit}((P^U_{arg,pet})^{UL}) - \text{logit}((P$

A new method to reconstruct quantitative food webs and nutrient flows from isotope tracer addition experiments.

Andrés López-Sepulcre[1,2,3*], Matthieu Bruneaux[2], Sarah M. Collins[4], Rana El-Sabaawi[5], Alexander S Flecker[6], and Steven A. Thomas[7]

[1]Department of Biology, Washington University in St. Louis, MO, USA
[2]Department of Biological and Environmental Sciences, University of Jyväskylä, Finland
[3]CNRS UMR 7618, Institute of Ecology and Environmental Sciences of Paris (iEES), Sorbonne Université, France
[4]Department of Zoology and Physiology, University of Wyoming, USA
[5]Department of Biology, University of Victoria, Canada
[6]Department of Ecology and Evolutionary Biology, Cornell University, USA
[7]School of Natural Resources, University of Nebraska-Lincoln, USA
[*]Corresponding author. E-mail: alopezsepulcre@wustl.edu

January 15, 2020

Supplementary Material S1. Implementation of the model for MCMC sampling

We sampled the posterior distributions of the model parameters using the Stan program and its R interface RStan (Carpenter et al., 2017; Stan Development Team, 2019). Stan implements Hamiltonian Monte Carlo (HMC) sampling, which allows for more efficient and reliable sampling of complex model posterior than a simple Metropolis-Hastings algorithm, especially as the dimension of the posterior increases.

Here, we present the model implementation in Stan by describing the data passed to the sampler, the priors used and the likelihood calculation. Our description is valid for either stream (UL and LL): we ran the model independently for both stream, and then combined the DIC values obtained for a given foodweb topology.

The model is based on solving numerically the system of differential equations describing the foodweb topology to calculate the trajectories of marked and unmarked nutrients based on a set of parameter values. The numerical solving of the differential equations is done using a simple discretization approach with a reasonably small dt value, and projecting the trajectories iteratively.

Data passed to Stan

The data passed to Stan for one stream comprises (using the notations from Table 1):

- a matrix of the same size as $\mathbf{\Psi_h}$ containing 0 and 1 values, and serving as a mask defining the directed connections existing between the foodweb compartments,
- the dt value of the time step used for the numerical solving of the system of differential equations describing the foodweb,
- for each transect, a vector describing the initial isotopic proportions $\mathbf{z}^{(s,0)}$ (i.e. the initial isotopic proportions for each compartment),
- for each transect, a table providing the observed data $z_{\text{obs},i}^{(s,t)}$ as one observation of proportion of marked tracer per row (with columns being the compartment observed and the time of observation),
- for each transect and for each inorganic nutrient compartment $i \in \mathcal{I}$, one table giving the pre-computed $n_i^{(t)}$ and $m_i^{(t)}$ values for every time step that will be used when solving the ODE system (those tables are calculated from the step functions based on the measured isotopic profiles for NH_4^+ and NO_3^-),
- shared across all transects of the stream, the initial biomass of each compartment (calculated from $x_{\text{obs},i}^{(s,t)}$) and its estimated standard deviation SD_i.

Sampled parameters and their priors

The parameters sampled by Stan are:

- all the non-zero uptake rates $\upsilon_{i,j}$ from compartment j to compartment i,

- all the non-zero loss rates λ_j from compartment j (i.e. for all organic compartments),
- the active portions π_i for the primary producers (CBOM, FBOM, epilithon, seston),
- the coefficient of variation η for observed isotopic ratios

The priors we used were:

$$\begin{aligned}
\upsilon_{i,j} &\sim \mathit{Half\text{-}Cauchy}(\mathit{scale} = 250) \text{ for input compartments } j \in \mathcal{I} \\
\upsilon_{i,j} &\sim \mathit{Beta}(\alpha = 1, \beta = 3, \mathit{scale} = 1) \text{ for all other uptake rates } \upsilon_{i,j} > 0 \\
\lambda_i &\sim \mathit{Beta}(\alpha = 1, \beta = 3, \mathit{scale} = 1) \\
\pi_i &\sim \mathit{Uniform}(0, 1) \text{ for all basal compartments } \pi_i < 1 \\
\eta &\sim \mathit{Half\text{-}Cauchy}(\mathit{scale} = 1)
\end{aligned}$$

with the following compartment-specific adjustments:

$$\begin{aligned}
\upsilon_{eudan,CBOM} &\sim \mathit{Beta}(\alpha = 1, \beta = 3, \mathit{scale} = 0.5) \\
\upsilon_{lepto,seston} &\sim \mathit{Beta}(\alpha = 1, \beta = 3, \mathit{scale} = 0.5)
\end{aligned}$$

where we defines X as following a scaled beta distribution $\mathit{Beta}(\alpha, \beta, \mathit{scale})$ if $\frac{X}{\mathit{scale}}$ follows a beta distribution $\mathit{Beta}(\alpha, \beta)$.

Likelihood calculation

Below is a pseudo-code for the calculation of the likelihood of a set of parameter values. It is applied for each transect of a stream.

1. Build the matrix $\mathbf{\Psi}$ using the parameter values to evaluate. The refractory portions $1 - \pi_i$ are included as separate, static compartments with no connection to any other compartment and no loss in an expanded $\mathbf{\Psi}$, i.e. only 0s on the corresponding rows and columns in the expanded $\mathbf{\Psi}$.
2. Build initial values of $\mathbf{n}^{(0)}$ and $\mathbf{m}^{(0)}$ using the mean of observed biomasses for compartments $\{\bar{x}_{\text{obs},1}, \bar{x}_{\text{obs},2}, \ldots, \bar{x}_{\text{obs},C}\}$, initial δ^{15}N values, and parameter values π (active portions of compartments).
3. Set $t = 0$. While $t \leq 40$ (40 days is the latest timepoint with observations):
   (a) $\mathbf{n}^{(t+dt)} = \mathbf{\Psi} \cdot \mathbf{n}^{(t)}$ and $\mathbf{m}^{(t+dt)} = \mathbf{\Psi} \cdot \mathbf{m}^{(t)}$ (Equation 1)
   (b) Set $t \leftarrow t + dt$
   (c) Update $n_i^{(t)}$ and $m_i^{(t)}$ for inorganic nutrient sources $i \in \mathcal{I}$ based on the pre-computed tables giving their values for each time point
4. Calculate the trajectories for biomasses $\mathbf{x}^{(t)}$ and proportions of marked tracer $\mathbf{z}^{(t)}$
   (a) $\mathbf{x}^{(t)} = \mathbf{m}^{(t)} + \mathbf{x}^{(t)}$

(b) $\mathbf{z}^{(t)} = \mathbf{m}^{(t)} \oslash \mathbf{x}^{(t)}$ (Equation 10)

5. Update $\mathbf{x}^{(t)}$ and $\mathbf{z}^{(t)}$ by merging active and refractory portions of split compartments into single observed compartments, using weighed averages according to π.

6. For each non-source compartment $i \notin \mathcal{I}$:

   (a) Set t_i the timepoints for which this compartment was sampled

   (b) Extract values $z_i^{t_i}$ calculated in 4.b.

   (c) Update likelihood assuming $z_{\text{obs},i}^{t_i} \sim \text{Gamma}^* \left(z_i^{(t)}, \eta\right)$ (Equation 12)

   (d) Extract values $x_i^{t_i}$ calculated in 4.a.

   (e) Update likelihood assuming $x_{\text{obs},i}^{t_i} \sim \text{TNorm}_{\text{lower}=0} \left(x_i^{(t_0)}, \text{SD}_i\right)$, where $x_i^{(t_0)}$ is the initial biomass of this compartment (i.e. the mean of observed biomasses for this compartment, potentially adjusted if the compartment is an active or refractory portion of an observed compartment), and SD_i is the standard deviation of observed biomasses for this compartment.

Supplementary Material S2. Supplementary tables and figures

Parameter	LL estimate	UL estimate
π_{epi}	0.136 [0.0114 – 0.274]	0.45 [0.238 – 0.727]
π_{CBOM}	0.19 [0.0187 – 0.439]	0.394 [0.0929 – 0.651]
π_{FBOM}	0.0775 [0.028 – 0.151]	0.0503 [0.0046 – 0.108]
π_{ses}	0.134 [0.0151 – 0.292]	0.35 [0.238 – 0.475]
$\upsilon_{\text{epi,NH4}}$	31.8 [20.7 – 48.4]	50.1 [36.5 – 68.7]
$\upsilon_{\text{CBOM,NH4}}$	14.4 [3.62 – 58.1]	41.3 [22.5 – 84.6]
$\upsilon_{\text{FBOM,NH4}}$	85.6 [44.8 – 138]	134 [75.4 – 216]
$\upsilon_{\text{ses,NH4}}$	0.0288 [0.0185 – 0.0503]	0.0146 [0.0113 – 0.019]
$\upsilon_{\text{epi,NO3}}$	0.00805 [0.000328 – 0.0409]	0.404 [0.0698 – 0.847]
$\upsilon_{\text{CBOM,NO3}}$	0.401 [0.0477 – 1.94]	1.08 [0.269 – 2.72]
$\upsilon_{\text{FBOM,NO3}}$	0.271 [0.0186 – 0.852]	0.248 [0.0121 – 0.79]
$\upsilon_{\text{ses,NO3}}$	0.000122 [0.00000865 – 0.000366]	0.0000311 [0.00000323 – 0.0000849]
$\upsilon_{\text{pet,epi}}$	0.0000587 [0.0000397 – 0.0000855]	0.000224 [0.0000902 – 0.000528]
$\upsilon_{\text{pse,epi}}$	0.00443 [0.00325 – 0.00629]	0.00344 [0.00232 – 0.00504]
$\upsilon_{\text{eud,CBOM}}$	0.0173 [0.00357 – 0.102]	0.00594 [0.00197 – 0.0182]
$\upsilon_{\text{phy,CBOM}}$	0.000449 [0.00011 – 0.00281]	0.0000896 [0.0000253 – 0.000363]
$\upsilon_{\text{tri,FBOM}}$	0.00197 [0.000667 – 0.00519]	0.0037 [0.00169 – 0.00888]
$\upsilon_{\text{lep,ses}}$	0.0555 [0.0341 – 0.0911]	0.0449 [0.0119 – 0.0801]
$\upsilon_{\text{arg,pet}}$	0.0122 [0.000531 – 0.0447]	0.0632 [0.012 – 0.142]
$\upsilon_{\text{arg,tri}}$	0.0216 [0.005 – 0.0773]	0.0183 [0.00553 – 0.0591]
$\upsilon_{\text{eut,tri}}$	0.119 [0.0217 – 0.38]	0.0817 [0.0194 – 0.236]
λ_{epi}	0.217 [0.131 – 0.343]	0.189 [0.126 – 0.264]
λ_{CBOM}	0.282 [0.0274 – 0.773]	0.165 [0.0668 – 0.382]
λ_{FBOM}	0.059 [0.0295 – 0.0894]	0.0882 [0.0528 – 0.17]
λ_{ses}	0.0708 [0.00454 – 0.224]	0.0168 [0.000626 – 0.0531]
λ_{pet}	0.013 [0.000584 – 0.0455]	0.0244 [0.000928 – 0.101]
λ_{pse}	0.0268 [0.0135 – 0.0445]	0.0296 [0.00931 – 0.056]
λ_{tri}	0.393 [0.085 – 0.775]	0.124 [0.017 – 0.334]
λ_{lep}	0.0306 [0.0046 – 0.085]	0.543 [0.396 – 0.835]
λ_{eud}	0.0336 [0.00216 – 0.13]	0.0416 [0.00781 – 0.133]
λ_{phy}	0.103 [0.0314 – 0.705]	0.167 [0.0649 – 0.584]
λ_{arg}	0.0612 [0.0184 – 0.166]	0.13 [0.0762 – 0.228]
λ_{eut}	0.0224 [0.00104 – 0.111]	0.0209 [0.000918 – 0.119]
η	0.096 [0.0878 – 0.105]	0.104 [0.0945 – 0.115]

Supplementary Table 1: Estimates of primary parameters (median and 95% credible interval) from the best model, $\mathbf{\Psi}_{100}$, for the closed closed canopy (LL) and open canopy (UL) streams.

Compartment i	Biomass $\hat{X}_i$ (mgN/m^2)	
	LL	UL
Epilithon	226 [192-258]	329 [279-382]
active	44.5 [34.7-57.4]	146 [83.8-246]
refractory	181 [152-207]	181 [89.9-251]
CBOM	879 [623-1100]	948 [528-1490]
active	72 [9.21-276]	266 [91.9-664]
refractory	793 [549-960]	660 [380-987]
FBOM	5410 [4990-6300]	5500 [5190-6100]
active	584 [259-1350]	518 [259-966]
refractory	4860 [4470-5120]	5000 [4700-5240]
Seston	0.663 [0.552-0.771]	0.244 [0.228-0.263]
active	0.0983 [0.0536-0.192]	0.0856 [0.061-0.12]
refractory	0.56 [0.457-0.637]	0.158 [0.128-0.186]
Petrophila	0.0908 [0.0333-0.418]	0.362 [0.0648-1.62]
Psephenus	7.54 [4.44-14.2]	18 [8.73-41.5]
Tricorythodes	2.2 [0.681-4.71]	8.58 [3.1-16]
Leptonema	0.19 [0.0548-0.995]	0.00692 [0.00161-0.015]
Eudaniela	41.2 [3.82-484]	41.5 [8.71-155]
Phylloicus	0.276 [0.0634-0.676]	0.148 [0.0281-0.37]
Argia	0.871 [0.0857-4.27]	1.45 [0.345-3.55]
Euthyplocia	11.9 [0.511-402]	35.9 [1.3-911]

Supplementary Table 2: Steady state compartment biomasses in mgN/m^2 estimated as the sum of the first two right eigenvectors of $\mathbf{\Psi}_{100}$.

Compartment i	Uptake $F_{i,\cdot}$ (mgN m^{-2} day^{-1})		Turnover time T_i' (days)	
	LL	UL	LL	UL
Epilithon	9.88	27.6	33.5	11.8
	[6.42-15]	[17.6-42.9]	[13.5-436]	[7.56-20.9]
	6.52	*24.9*	*35.71*	*15.38*
CBOM	17.3	46.4	23.4	15.8
	[3.05-75.9]	[16.9-108]	[4.5-229]	[5.71-66.6]
	6.52	*24.9*	*35.71*	*15.38*
FBOM	35.2	49.3	213	222
	[17.5-62.3]	[27-81.6]	[83.8-851]	[84.5-2390]
	128	*244*	*29.41*	*36.71*
Seston	0.0127	0.00541	61.8	45.2
	[0.00717-0.0233]	[0.00386-0.00773]	[22.1-533]	[32-66.4]
	0.55	*0.222*	*21.28*	*16.13*
Petrophila	0.0026	0.0319	34	10.5
	[0.0019-0.00366]	[0.01-0.113]	[15.7-145]	[5.73-25.1]
	0.012	*0.111*	*12.6*	*11.6*
Psephenus	0.196	0.505	37.3	33.7
	[0.154-0.269]	[0.264-0.952]	[22.5-74.2]	[17.8-107]
	0.263	*0.459*	*19.7*	*30*
Tricorythodes	1.16	1.92	1.81	4.25
	[0.412-2.79]	[0.943-4.01]	[1.03-3.76]	[2.14-8.32]
	0.392	*2.83*	*6.26*	*3.78*
Leptonema	0.00549	0.00391	32.7	1.84
	[0.0027-0.0112]	[0.00106-0.00664]	[11.8-217]	[1.2-2.52]
	0.01	*0.296*	*23.7*	*10.9*
Eudaniela	1.17	1.54	29.8	24
	[0.273-5.04]	[0.513-5.45]	[7.72-464]	[7.51-128]
	4.3	*2.7*	*173*	*149*
Phylloicus	0.0273	0.0241	9.75	6
	[0.00726-0.22]	[0.00571-0.0968]	[1.42-31.8]	[1.71-15.4]
	0.11	*0.108*	*7.8*	*27.3*
Argia	0.049	0.181	16.3	7.7
	[0.0131-0.124]	[0.0688-0.367]	[6.03-54.3]	[4.39-13.1]
	0.02	*0.02*	*25.7*	*13.6*
Euthyplocia	0.254	0.709	44.6	47.9
	[0.0516-0.676]	[0.159-1.41]	[8.98-962]	[8.42-1090]
	0.3	*0.8*	*104.2*	*93.6*

Supplementary Table 3: Flux and turnover time estimates and 95% credible intervals. Estimates from Collins et al. (2016) are shown in italics for comparison.

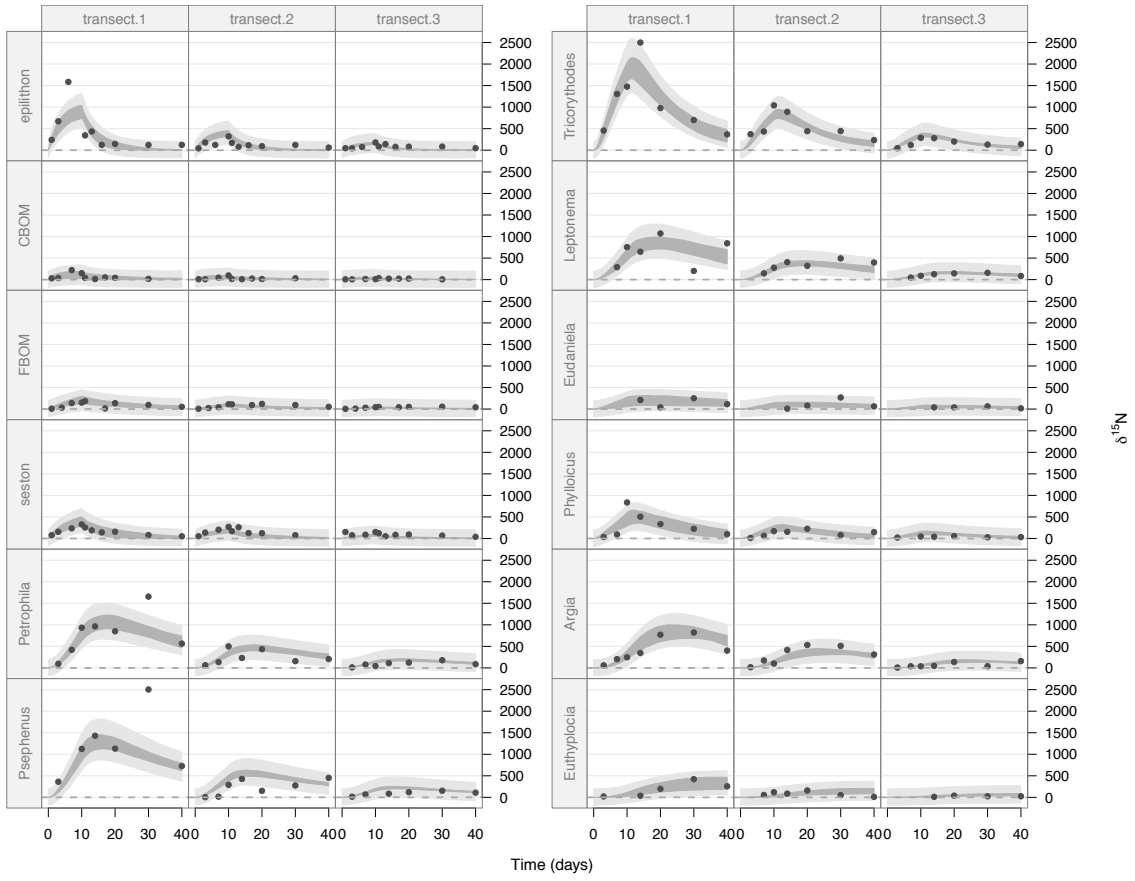

(a) Lower La Laja (LL)

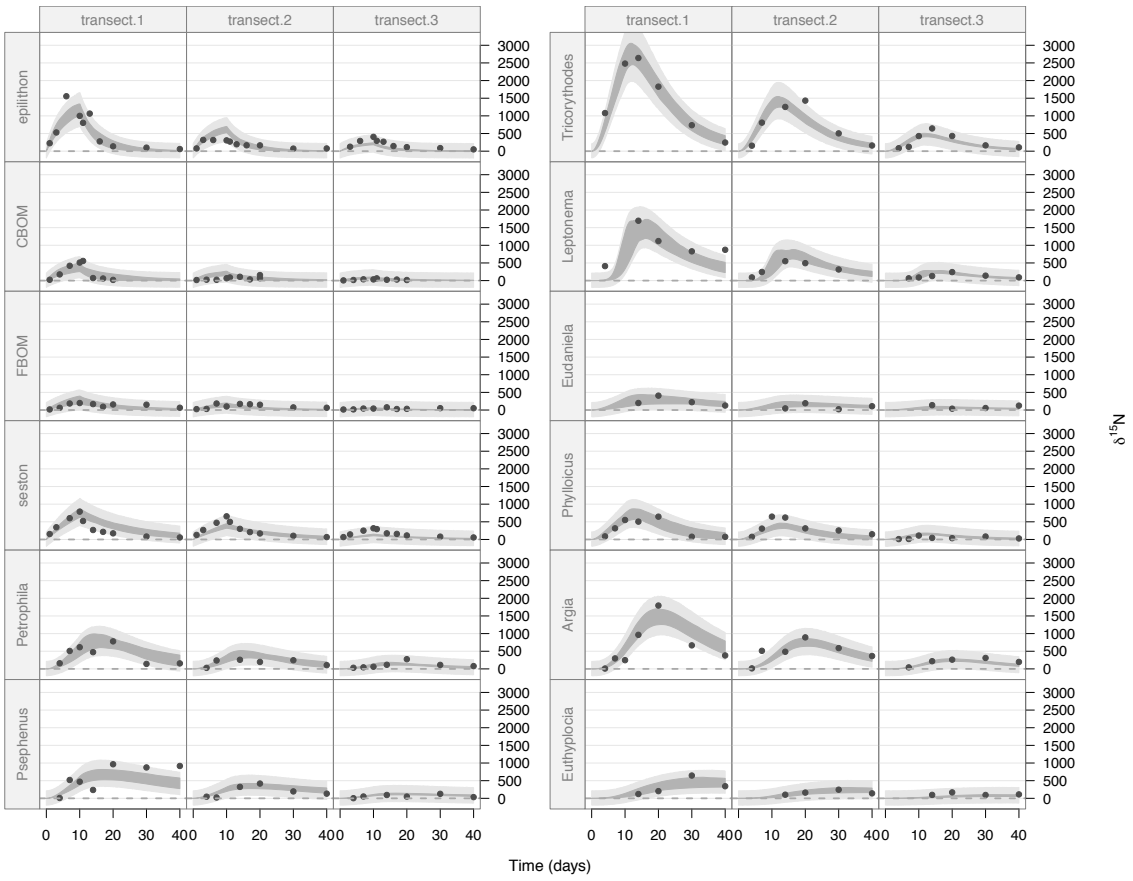

(b) Upper La Laja (UL)

Supplementary Figure 1: Model fit for comparing data with credible and prediction envelopes (δ^{15}N). Solid dots are observed data; dark grey envelopes are 95% credible intervals; and light grey envelopes are 95% prediction intervals.

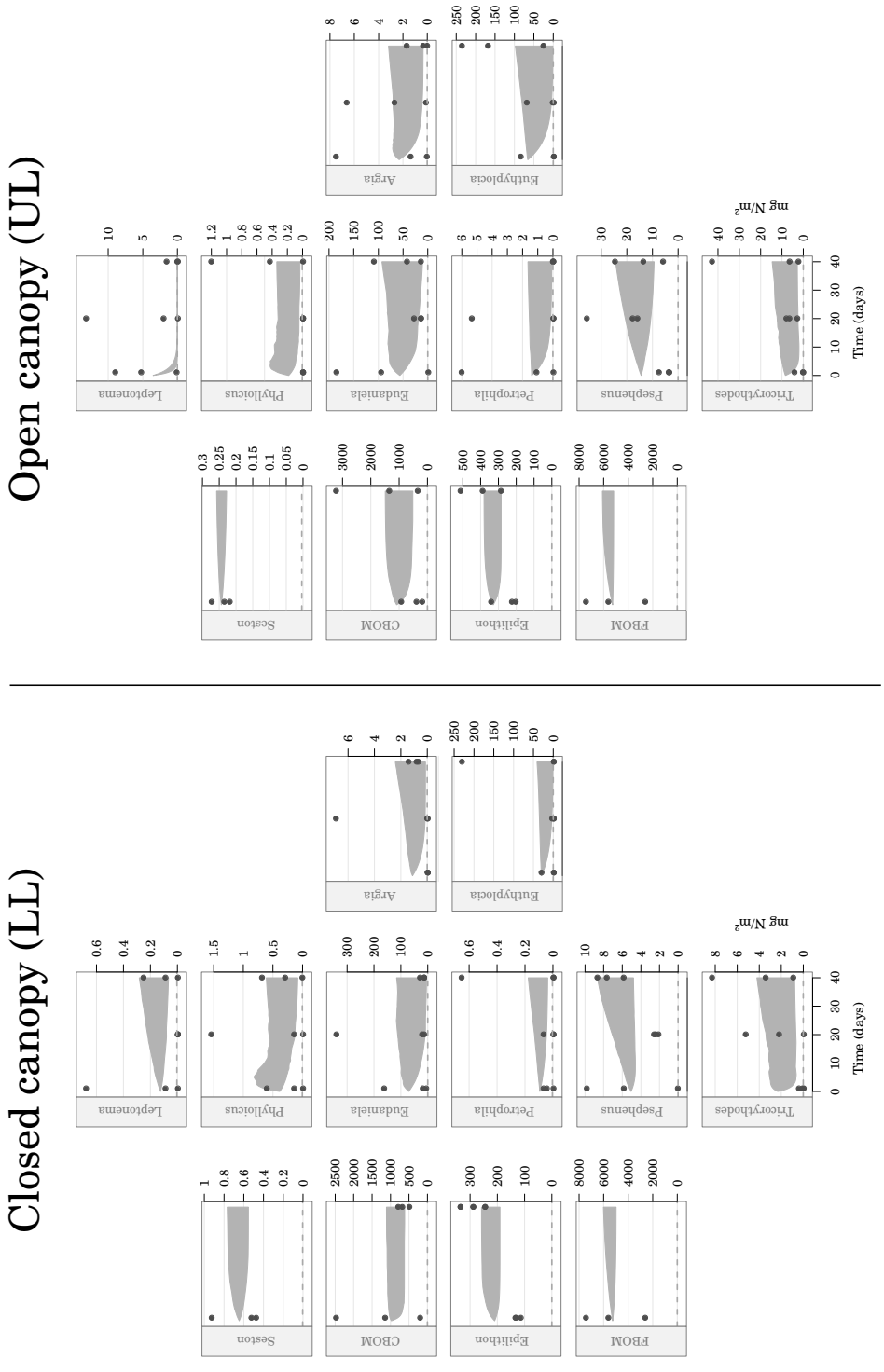

Supplementary Figure 2: Model fit for comparing data with credible envelopes (N biomasses). Solid dots are observed data; dark grey envelopes are 95% credible intervals. In the model used, for each stream (LL and UL), biomass data from the three transects were pooled and averaged to define common starting biomasses for all three transects, which is why all transects within a stream share the same biomass trajectories for a given compartment.

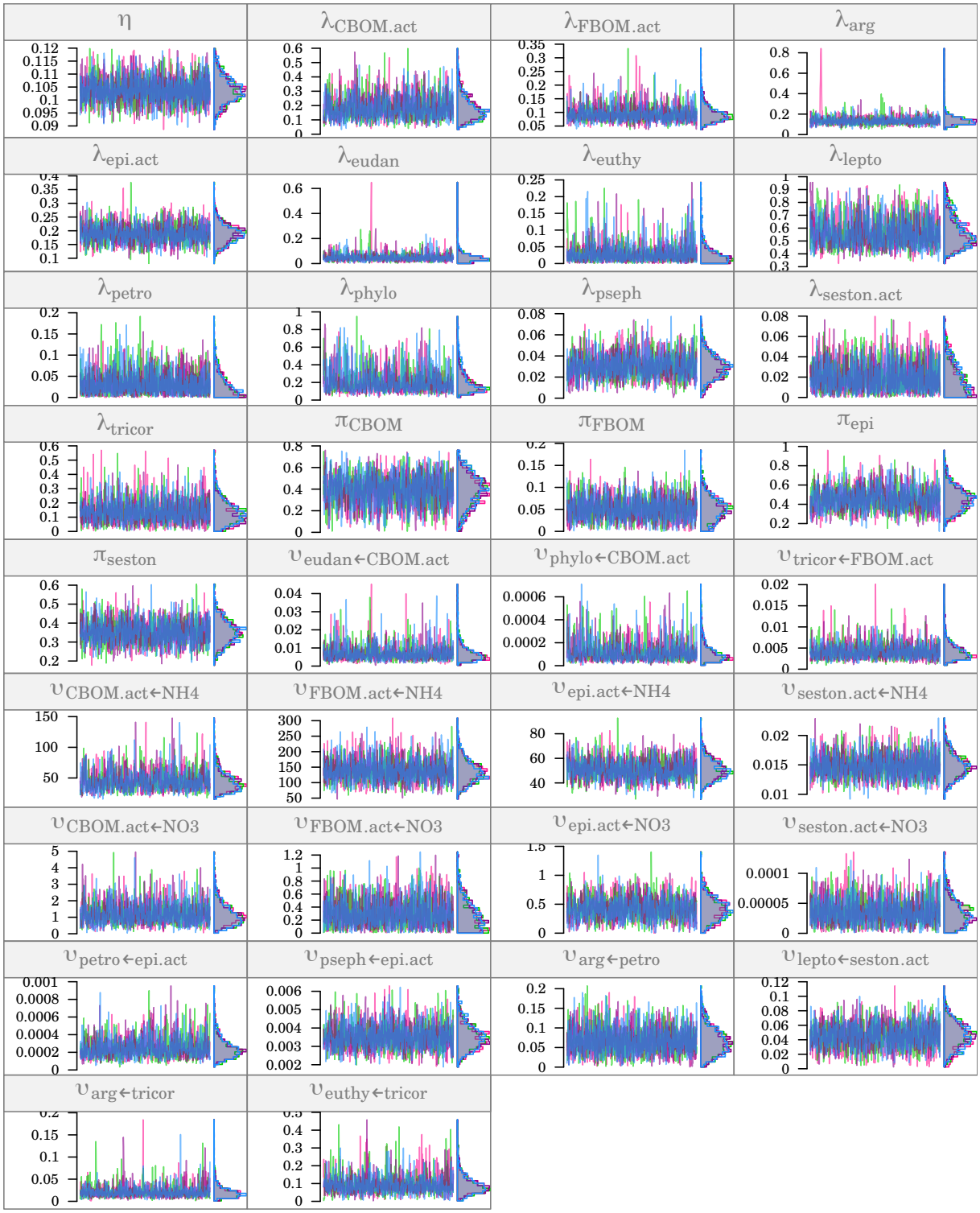

(a) Lower La Laja (LL)

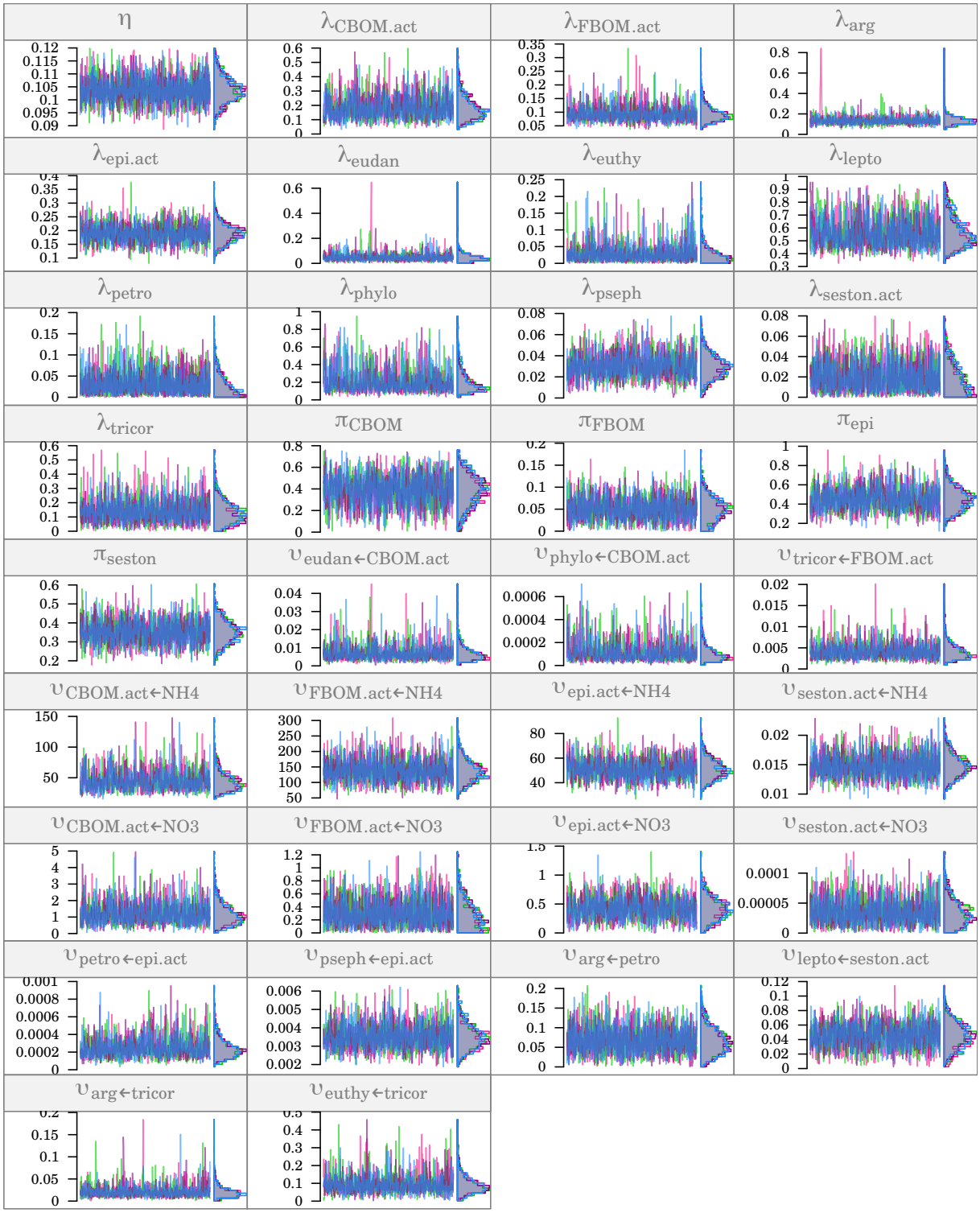

(b) Upper La Laja (UL)

Supplementary Figure 3: MCMC chains of primary parameters for the the final model fits. Four chains were run for each model. For each chain, the trace in the main panels and the density plot in the side panel are shown with matching color.